

Central Lancashire Online Knowledge (CLoK)

Title	Super-slowly rotating Ap (ssrAp) stars: New spectroscopic observations
Type	Article
URL	https://knowledge.lancashire.ac.uk/id/eprint/57518/
DOI	https://doi.org/10.1051/0004-6361/202556104
Date	2025
Citation	Mathys, G., Holdsworth, D. L. orcid iconORCID: 0000-0003-2002-896X, Giarrusso, M., Kurtz, Donald Wayne, Catanzaro, G. and Leone, F. (2025) Super-slowly rotating Ap (ssrAp) stars: New spectroscopic observations. Astronomy & Astrophysics, 703. A102. ISSN 0004-6361
Creators	Mathys, G., Holdsworth, D. L., Giarrusso, M., Kurtz, Donald Wayne, Catanzaro, G. and Leone, F.
1	Catalizato, of alla Ecolic, i.i.

It is advisable to refer to the publisher's version if you intend to cite from the work. https://doi.org/10.1051/0004-6361/202556104

For information about Research at UCLan please go to http://www.uclan.ac.uk/research/

All outputs in CLoK are protected by Intellectual Property Rights law, including Copyright law. Copyright, IPR and Moral Rights for the works on this site are retained by the individual authors and/or other copyright owners. Terms and conditions for use of this material are defined in the http://clok.uclan.ac.uk/policies/



Super-slowly rotating Ap (ssrAp) stars: New spectroscopic observations

G. Mathys^{1,*}, D. L. Holdsworth^{2,3}, M. Giarrusso⁴, D. W. Kurtz^{5,6}, G. Catanzaro⁴, and F. Leone^{7,4}

- ¹ European Southern Observatory, Alonso de Cordova 3107, Vitacura, Santiago, Chile
- ² South African Astronomical Observatory, PO Box 9, Observatory 7935, Cape Town, South Africa
- School of Physics, Engineering and Technology, University of York, Heslington, York YO10 5DD, UK
- ⁴ INAF–Osservatorio Astrofisico di Catania, via S. Sofia 78, 95123 Catania, Italy
- ⁵ Centre for Space Research, North-West University, Mahikeng 2745, South Africa
- ⁶ Jeremiah Horrocks Institute, University of Central Lancashire, Preston PR1 2HE, UK
- Dipartimento di Fisica e Astronomia, Sezione Astrofisica, Università di Catania, Via S. Sofia 78, I-95123 Catania, Italy

Received 25 June 2025 / Accepted 4 September 2025

ABSTRACT

Context. The rotation periods of Ap stars range over five to six orders of magnitude. The origin of their differentiation remains unknown.

Aims. We carry out a systematic study of the longest period Ap stars to gain insight into their properties.

Methods. We analysed newly obtained spectra of a sample of super-slowly rotating Ap (ssrAp) star candidates identified by a TESS photometric survey to confirm that their projected equatorial velocity, $v \sin i$, is consistent with (very) long rotation periods; to obtain a first determination of their magnetic fields; and to test their binarity.

Results. The value of $v \sin i$ in 16 of the 18 studied stars is low enough for them to have moderately to extremely long rotation periods. All stars but one are definitely magnetic; for five of them, the magnetic field was detected for the first time. Another set of five new stars with resolved magnetically split lines were discovered. Five of the stars that were not previously known to be spectroscopic binaries were found to show radial velocity variations, and in one of them, lines from both components were observed.

Key words. stars: chemically peculiar – stars: magnetic field – stars: oscillations – stars: rotation

1. Introduction

The existence of a substantial population of stars with rotation periods of months to centuries among early-type stars with radiative envelopes and large-scale organised magnetic fields has become increasingly well established in the past decade (Mathys 2017; Shultz et al. 2018). These stars represent the extreme tail of a rotation rate distribution that spans five to six orders of magnitude, from less than one day to centuries. The spectral types of the magnetic stars with radiative envelopes range from early F to O. They include, in order of increasing temperature, chemically peculiar F, A, and B stars (Fp, Ap, and Bp stars, often referred to collectively as Ap stars); magnetic early B stars (with spectral types ranging from B5 to B0); and magnetic O stars. All three groups show a similar distribution of the rotation periods (Shultz et al. 2018). However, while there is evidence for some loss of angular momentum due to magnetospheric braking on the main sequence for the two hotter groups (Shultz et al. 2019), whether the same mechanism can account for the occurrence of super-slow rotation in Ap stars has not been established yet. The identification of the relevant processes has, until now, been hampered by the lack of relevant observational constraints. The need for additional observations leading to better characterisation of possible connections between rotation, magnetic field, and other physical properties in order to guide theoretical developments is clear, but the most relevant missing elements of information have not been specifically identified yet. In these conditions, focusing

on the group of stars showing the most extreme slow rotation appears as one of the most promising approaches to distinguish other properties related to spin rate differentiation.

Early knowledge of extremely slow rotation in Ap stars was strongly biased towards strongly magnetic stars, since the identification of long periods was mostly a by-product of the interest in studying stars showing resolved magnetically split lines, whose magnetic fields can be determined in a particularly complete, assumption-free and model-independent manner (see below for more details). Accordingly, systematic surveys were carried out to search for such stars (Preston 1971; Mathys et al. 1997; Freyhammer et al. 2008; Elkin et al. 2012; Chojnowski et al. 2019), many of which were subsequently studied in greater detail (see in particular Mathys 2017; Giarrusso et al. 2022). By contrast, weakly magnetic Ap stars that potentially have (very) long periods received little attention. This difference introduced a potential bias in the knowledge of (very) slow rotation in Ap stars, at best preventing potential connections between magnetic properties and rotation rate from being investigated.

To address this bias, we undertook a systematic search (Mathys et al. 2020, 2022, 2024b) based on the photometric survey carried out with the Transiting Exoplanet Survey Satellite (TESS; Ricker et al. 2015) that allowed us to identify 144 superslowly rotating Ap star candidates. These identifications are based on the assumption that Ap stars that do not show photometric variations other than due to pulsation over the duration of a TESS cycle (27 d) have, with a high probability, a rotation period $P_{\rm rot} > 50$ d. This value is, by (arbitrary) definition, the lower limit

^{*} Corresponding author: gmathys@eso.org

of super-slow rotation (Mathys 2020). However, spectroscopic observations at sufficient resolution are necessary to confirm the photometric identification of ssrAp stars. In particular, it is necessary to verify that the Ap classification of the candidate is correct and that its spectral lines do not show Doppler broadening inconsistent with rotation periods of 50 d or longer.

For about half of the TESS-identified ssrAp star candidates, such confirmation is available in the literature. For the other half, we undertook a systematic programme to acquire a spectrum of each star at medium-high to high resolving power (40 000 $\leq R \leq 115$ 000). In addition to peculiarity and rotational (non)-broadening confirmation, these observations allow the derivation of preliminary constraints on the magnetic fields of the targets. The results of the analysis of spectra obtained as part of this project for a first batch of 27 ssrAp star candidates were presented by Mathys et al. (2024a) (herafter M24). Seventeen of these targets proved to be Ap stars with projected equatorial velocities consistent with super-slow rotation, or at least with moderately long rotation periods (20 d $\leq P_{\rm rot} \leq 50$ d). Misclassification was probably responsible for most of the broader-lined stars.

The present paper is based on a second series of spectra that were obtained more recently as part of this project. Again, a minority among them show line broadening inconsistent with super-slow rotation. We postpone their discussion to a later work and focus exclusively on the sharpest-lined Ap stars of the studied sample.

The observations analysed in this work are described in Sect. 2. The methods used to extract information from them are introduced in Sect. 3. Section 4 presents the results of our measurements, which are summarised in Sect. 5. Graphical illustration and tabular material related to the data discussed in Sects. 2 and 4 are included in Appendix A. The conclusion (Sect. 6) gives an overview of the current status of the project and of the forthcoming steps that we plan to carry out.

2. Observations

In this paper, we present the results of the analysis of 18 stars that do not show broad spectral lines. New spectra have been obtained for 17 of them. Fifteen of these 17 stars were identified as ssrAp star candidates in our TESS-based survey (Mathys et al. 2020, 2022, 2024b). The other two, HD 117290 and HD 143487, had been reported by Freyhammer et al. (2008) to have resolved magnetically split lines, which is suggestive of (very) slow rotation.

For 11 of the 15 ssrAp star candidates, prior to our study, there were no published measurements of the mean magnetic field modulus, $\langle B \rangle$, or of the mean quadratic magnetic field, $\langle B_{\rm q} \rangle$, no value of the rotation period, $P_{\rm rot}$, and no determination of the projected equatorial velocity, $v \sin i$, with a resolution sufficient to assess critically the occurrence of super-slow rotation. Measurements of the mean longitudinal magnetic field, $\langle B_z \rangle$, of four of them had been obtained at a few epochs, but the time sampling provided was insufficient for setting meaningful constraints on the rotation period. While these measurements confirm that the stars are detectably magnetic, their sensitivity to the observational geometry limits their usability for characterisation of the intrinsic field strengths.

Of the 18 stars analysed in this present study, four had more information available in the literature. These four are HD 8441, with determinations of $P_{\rm rot}$, $v \sin i$, and $\langle B_z \rangle$ (but with $\langle B_q \rangle$ below the detection threshold); HD 221568 ($P_{\rm rot}$, $v \sin i$, $\langle B_z \rangle$, and a quantity that is essentially $\langle B_q \rangle$, at one epoch); HD 76460; and HD 110274 (both of them $\langle B \rangle$). More details, including the relevant references, are given in Sect. 4.

We recorded new spectra of 17 stars. Lower resolution ($R \sim 40\,000$ against $R \sim 115\,000$) spectroscopic observations of four of them had already been discussed in M24: HD 11187, HD 17330, HD 203922, and BD+35 5094. In addition, we complement the study of HD 151860 from M24 with the analysis of a UV-Visual Echelle Spectrograph (UVES) spectrum from the European Southern Observatory (ESO) Archive.

The new observations presented here were obtained with either the High Accuracy Radial velocity Planet Searcher for the Northern Hemisphere (HARPS-N; Cosentino et al. 2012) at the Telescopio Nazionale Galileo (TNG) or the Southern African Large Telescope High Resolution échelle Spectrograph (SALT-HRS; Bramall et al. 2010). The former covers the wavelength range 3830–6930 Å with a resolving power of $R \sim 115000$; the latter was used in High Resolution (HR) mode to achieve $R \sim 45\,000$ from 3700 Å to 8900 Å. The data obtained with these instruments were complemented with spectra recorded with UVES (Dekker et al. 2000; $R \sim 107\,000$ over 4960–7070 Å) fed by Unit Telescope 2 (UT2) of the ESO Very Large Telescope (VLT), HARPS (Mayor et al. 2003; $R \sim 115000$ over 3800–6900 Å) fed by the ESO 3.6-m telescope, and the Fiber-fed Extended Range Optical Spectrograph (FEROS) (Kaufer et al. 1999; $R \sim 48\,000$ over 3530–9220 Å) fed by the ESO 2.2-m telescope. The reduced HARPS and UVES spectra were retrieved from the ESO Archive.

The two 2008 UVES spectra of HD 110274 (JD 2454523 and 2454535), the 2008 UVES spectrum of HD 117290 (JD 2454515), all four UVES spectra of HD 143487 and the single UVES spectrum of HD 151860 were acquired as long time series (up to ~2 h) of short integrations (~60–80 s) to study line profile variations due to pulsation. These individual exposures were averaged in the reduction process to produce the spectra analysed here. The FEROS spectra were recorded by a team including DWK and GM (Freyhammer et al. 2008; Elkin et al. 2012) as part of a systematic survey of cool Ap stars from a list compiled by Martinez (1993). Whenever the corresponding reduced spectra were available in the ESO Archive, we used them for the present study; otherwise, we used our original reductions. (All the observation dates are fully specified in Table A.1. We have uploaded all the reduced spectra to the CDS.)

For the 13 stars that were not studied in M24, 30 Å long portions of the spectra are shown in Figs. A.1 to A.3. The format is similar to that of Figs. A.1 to A.5 of M24, with the stars sorted in order of increasing effective temperature, so that the two sets of observations can be easily compared. The main transitions responsible for a number of lines are identified, and the way in which their intensities evolve along the temperature sequence can be traced, as described in M24. Remarkable chemical peculiarities can also be spotted, such as the large intensities of the Nd III λ 6145.1 Å and Pr III λ 6160.2 Å lines in HD 143487 and HD 138777, which are indicative of considerable overabundances of these elements.

The Fe II λ 6149.2 Å line is resolved into its magnetically split components in 11 of the 18 studied stars, which allows their mean magnetic field modulus $\langle B \rangle$ (that is, the line intensity weighted over the visible stellar hemisphere of the modulus of the magnetic vector) to be determined. This resolution is reported here for the first time for five stars: HD 119794, HD 138777, HD 192686, HD 221568, and BD+52 3124. The presence of resolved magnetically split lines in the other six stars had already been announced by Freyhammer et al. (2008), Elkin et al. (2012), and M24. A blown-up portion of the spectra of two of the eleven stars with resolved magnetically split lines,

HD 151860 and HD 203932, including the Fe II λ 6149.2 Å line, is shown in Fig. 2 of M24 (we note that both stars were mistakenly assigned the same TIC number in this figure; the correct identification of HD 151860 is TIC 170419024). Here we present the same spectral region in Fig. A.4 for the remaining nine stars with resolved magnetically split lines.

3. Analysis

We present the results of the analysis of 35 spectra of the 18 studied stars. This includes the determination of the following parameters: the radial velocity $v_{\rm r}$ (except for some FEROS spectra whose wavelength calibration is inadequate for this purpose), the mean magnetic field modulus $\langle B \rangle$ (only for the 27 spectra in which the Fe II λ 6149.2 Å line is resolved into its magnetically split components), the mean quadratic magnetic field $\langle B_{\rm q} \rangle$ (the square root of the sum of the mean square magnetic field modulus and of the mean square longitudinal magnetic field; see Mathys 1995), and the upper limit of the projected equatorial velocity $v \sin i$.

Knowledge of each of these parameters serves different purposes. The magnetic field is a fundamental property that contributes to the definition of the evolution of the star. Its consideration is of particular relevance for the understanding of the processes that affect the stellar rotation, given its potential to affect the latter through magnetic braking. Furthermore, studying the field variability represents the most effective way to constrain reliably rotation periods of the order of years to decades. Indeed, the variation amplitudes are generally large compared to the measurement uncertainties, and $\langle B \rangle$ and $\langle B_q \rangle$ determinations over long time spans are less subject to systematic instrumental effects and instrument to instrument calibration differences than $\langle B_z \rangle$ or photometric measurements (see Mathys 2020, for more details). Whenever $\langle B \rangle$ can be determined, that is the most valuable piece of information that we can extract from our analysis. For stars that do not show resolved magnetically split lines, $\langle B_q \rangle$ represents a suitable substitute that allows one to build a larger sample for statistical study of the distribution of the magnetic field strengths and of the possible correlations between magnetic field strength and rotation period. For spectra in which both $\langle B \rangle$ and $\langle B_{\mathbf{q}} \rangle$ can be derived, comparison between the two values is valuable to characterise their overall connection so that statistical studies can be meaningfully carried out with a mix of both in the sample, depending on their respective availability.

The main motivation for determination of the upper limit of $v \sin i$ is to identify in the sample those stars that can plausibly have periods $P_{\rm rot} > 50\,\rm d$ and hence that are worth re-observing at multiple epochs as part of the quest for characterisation and undestanding of super-slow rotation in Ap stars. A first estimate is adequate for this purpose, without requiring the additional effort for accurate untangling of the various contributions to the Doppler-like component of the line broadening (see below). The procedure by which $\langle B_{\rm q} \rangle$ is determined represents a convenient means to this effect. The consistency between the $v \sin i$ upper limit derived in this way and the difference between the observed width of the Fe I λ 5434.5 Å magnetic null line and its instrumental and thermal broadening was illustrated in Fig. 4 of M24.

The possible existence of a connection between rotation and binarity among Ap stars may potentially reflect the existence of a merger channel of Ap star formation (Ferrario et al. 2009; Tutukov & Fedorova 2010) that is at the same time responsible for super-slow rotation (Mathys 2017). Accordingly, multiepoch determinations of the radial velocity of ssrAp stars is a sensible undertaking. Similar to the $\langle B \rangle$ and $\langle B_q \rangle$ measurements,

the $v_{\rm r}$ values that we determine here often represent a first reference to which future values will be compared. More generally, their (very) sharp lines allow ssrAp stars to have their radial velocities determined with exquisite accuracy. This opens an opportunity to study some of the widest binaries containing an Ap component.

The determination of v_r is straightforward. The methods applied for determination of $\langle B \rangle$, $\langle B_q \rangle$, and $(v \sin i)_{max}$ were described in detail in M24.

The value of the mean magnetic field modulus is computed from the wavelength separation of the components of the Fe II λ 6149.2 Å doublet by application of the formula

$$\lambda_{\rm r} - \lambda_{\rm b} = g \, \Delta \lambda_{\rm Z} \, \langle B \rangle, \tag{1}$$

where $\lambda_{\rm r}$ and $\lambda_{\rm b}$ are the wavelengths of the red and blue line components, respectively; g = 2.70 is the Landé factor of the split level of the transition; $\Delta \lambda_Z = k \lambda_0^2$, with $k = 4.67 \times 10^{-13} \text{ Å}^{-1} \text{ G}^{-1}$; and $\lambda_0 = 6149.258 \,\text{Å}$ is the nominal wavelength of the transition. The wavelengths are expressed in Angströms and the magnetic field in Gauss. The wavelengths are measured by fitting simultaneously a Gaussian to each of the two split components; a third Gaussian is added to the fit for the blending line affecting the blue wing of the Fe II λ 6149.2 Å line when its contribution can significantly impact the derived values of λ_b and λ_r . The uncertainties of the derived $\langle B \rangle$ values are estimated by comparing the analysed spectra with those of stars well observed over a full rotation cycle (or at least over a wide enough range of phases), for which the uncertainties are given by the scatter of the individual measurements around a smooth variation curve. This procedure was discussed more extensively by Mathys et al. (1997).

For determination of the mean quadratic magnetic field, the observed line widths in natural light (Stokes I) are characterised by the second-order moments $R_I^{(2)}(\lambda_I)$ of their profiles about their centre of gravity λ_I . Following Mathys & Hubrig (2006), a sample of lines are analysed to untangle three contributions to their broadening by performing a multiple least-squares fit of the form

$$R_I^{(2)}(\lambda_I) = a_1 \frac{1}{5} \frac{\lambda_0^2}{c^2} + a_2 \frac{3S_2 + D_2}{4} \Delta \lambda_Z^2 + a_3 W_\lambda^2 \frac{\lambda_0^4}{c^4}.$$
 (2)

In this equation, W_{λ} is the equivalent width of the line, and S_2 and D_2 are atomic parameters characterising the Zeeman pattern of the considered transition. For details about these parameters as well as about the definition and actual measurement of $R_I^{(2)}(\lambda_I)$, see Mathys (2017). The fit coefficients a_1 , a_2 , and a_3 are related to the physical parameters of interest in the present context.

The third term on the right-hand side of Eq. (2) represents the intrinsic line width (Mathys & Hubrig 2006). It does not provide any useful information for our purpose, but it must be taken into account to avoid overestimating the other two terms. Magnetic broadening is accounted for by the second term; the mean quadratic magnetic field is given by the a_2 fit coefficient: $\langle B_{\rm q} \rangle = \sqrt{a_2}$. Its formal uncertainty is computed from the standard deviation $\sigma(a_2)$, which corresponds to the line-to-line scatter about the best fit regression. Finally, the first term on the right-hand side of Eq. (2) includes all the contributions to the line width that have the same wavelength dependence as the Doppler effect. This includes the rotational and thermal broadening, any other Doppler broadening of stellar origin (for instance, due to microturbulence or to stellar oscillations), and instrumental broadening. Accordingly, an upper limit of the projected equatorial velocity can be derived from consideration of the a_1 fit coefficient:

$$v \sin i \le (a_1 - a_{\text{inst}} - 1.474 \times 10^{-3} T_{\text{eff}})^{1/2},$$
 (3)

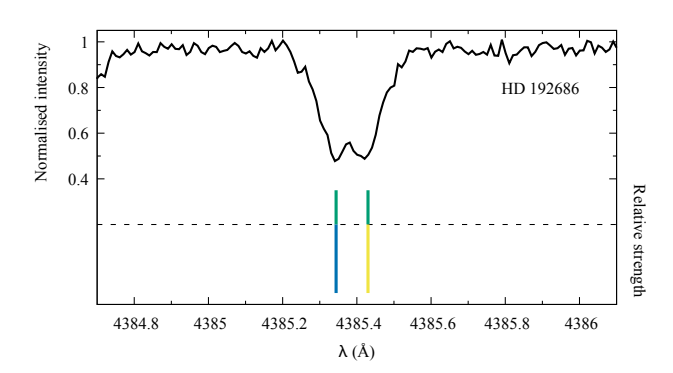


Fig. 1. Portion of the spectrum of HD 192686 showing the Fe II λ 4385.4 Å line. The Zeeman pattern of this line, a doublet, is illustrated below the spectrum. The amplitude of the splitting corresponds to the measured value of the mean magnetic field modulus, $\langle B \rangle = 3573~G$. The length of each vertical bar is proportional to the relative strength of the corresponding line component. The π components appear above the horizontal line (in green), the σ_+ and σ_- components below it (in blue and yellow, respectively).

where $T_{\rm eff}$ is the effective temperature of the analysed star. In this equation, the contribution of the instrumental profile is $a_{\rm inst} = 40.02\,{\rm km^2\,s^{-2}}$ (SALT-HRS), $a_{\rm inst} = 35.17\,{\rm km^2\,s^{-2}}$ (FEROS), $a_{\rm inst} = 6.70\,{\rm km^2\,s^{-2}}$ (UVES), or $a_{\rm inst} = 6.13\,{\rm km^2\,s^{-2}}$ (HARPS and HARPS-N; the $1.23\,{\rm km^2\,s^{-2}}$ value given in M24 was mistaken). As for $\langle B_{\rm q} \rangle$, we adopt $\sigma(a_1)$ as the formal uncertainty of the upper limit of $v\sin i$. It reflects the line-to-line scatter in the regression analysis that is carried out to derive the values of $\langle B_{\rm q} \rangle$ and $(v\sin i)_{\rm max}$ but does not account for possible systematic errors that may affect the determination of these quantities.

The measurement procedures sketched above have been discussed more extensively in M24. This reference also includes several examples that illustrate the approach followed and its potential shortcomings. The procedure that we use for determination of the mean quadratic magnetic field and of the upper limit of the projected equatorial velocity is best suited for study of a statistical sample of stars. Admittedly, detailed modelling of individual stars may yield more accurate results since, for instance, the micoturbulence contribution to the Doppler line broadening can be untangled from other effects. But its application is much more time-consuming and accordingly inappropriate for the purpose of obtaining preliminary constraints on the properties of a rather large set of stars in order to select the most interesting targets for a full multi-epoch study. Once observations providing a good sampling of the rotation cycle of a given star have been acquired, it will be much more meaningful to compute a detailed model.

4. Measurement results

The results of the new measurements reported in this paper are summarised in Table A.1. Below, we discuss them on a star-by-star basis.

4.1. TIC 32259138 (HD 138777)

The Fe II λ 6149.2 Å line is resolved into its magnetically split components in the SALT-HRS spectrum of HD 138777 analysed here. From this splitting, we derived a value $\langle B \rangle = 4698\,\mathrm{G}$ of the mean magnetic field modulus. As in numerous other Ap stars with resolved magnetically split lines, the blue component

of Fe II λ 6149.2 Å is significantly affected by an unidentified blending line. Accordingly, we estimate the uncertainty of $\langle B \rangle$ to be of the order of 100 G. Taking into account the involved uncertainties, the ratio between the value of the mean magnetic field modulus and that of the mean longitudinal magnetic field reported by Romanyuk et al. (2017), $\langle B_z \rangle = 2.1$ kG, is within the typical range (see Sect. 5.2 of Mathys 2017, for details).

The precision of the derived value of the mean quadratic field (from the analysis of Fe I lines), $\langle B_{\rm q} \rangle = 5600 \pm 300 \, {\rm G}$, ranks among the best ones achieved from SALT-HRS spectra. The $\langle B_{\rm q} \rangle$ determination did not reveal any significant rotational broadening. This lends strong support to the conclusion that HD 138777 is an ssrAp star.

Within uncertainties, the value of the radial velocity that we derived, $v_r = -43.72 \pm 0.12 \,\mathrm{km \, s^{-1}}$ is consistent with the values of Romanyuk et al. (2017) ($v_r = -46.3 \pm 2.7 \,\mathrm{km \, s^{-1}}$) and of Steinmetz et al. (2020) ($v_r = -47.7 \pm 2.9 \,\mathrm{km \, s^{-1}}$). Thus, there is no indication of binarity for HD 138777.

4.2. TIC 88202438 (HD 192686)

The hottest star of the present sample, HD 192686, was observed with HARPS-N. The Fe II λ 6149.2 Å line is resolved into its magnetically split components. Unusually, the red component is heavily blended, by an unidentified line. This hampers the determination of the mean magnetic field modulus from this line. Instead, we used the Fe II λ 4385.387 Å line to derive the value of this field moment. This line is blend-free in HD 192686 (but in general not in cooler stars). It arises from the transition $b^4P_{1/2}$ – $z^4D_{1/2}^{\circ}$ while the transition responsible for Fe II $\lambda 6149.2 \,\text{Å}$ is $b^4D_{1/2} - z^4P_{1/2}^{\circ}$. Hence the two lines have essentially the same Zeeman pattern, with a Landé factor q of the ${}^4D_{1/2}$ levels not significantly different from zero, and with g = 2.70(Fe II λ 6149.2 Å) and q = 2.68 (Fe II λ 4385.4 Å) for the ${}^{4}P_{1/2}$ levels. These lines are both pure doublets, in which the two π components each are shifted from the line centre by the same amount as each of the σ components. However, for a given magnetic field strength, this shift is greater in the Fe II λ 6149.2 Å line than in the Fe II λ 4385.4 Å line, because of the quadratic dependence of the Zeeman effect on the wavelength. The observed splitting of Fe II λ 4385.4 Å in HD 192686 is illustrated in Fig. 1. From its consideration, we derived a value $\langle B \rangle = 3573 \pm 50 \,\mathrm{G}$ for the mean magnetic field modulus.

Given the high effective temperature of HD 192686, Fe II lines were used to diagnose its mean quadratic magnetic field, $\langle B_{\rm q} \rangle = 4730 \pm 230$ G. Our analysis did not detect any significant rotational broadening. This supports the view that HD 192686 is an ssrAp star. The derived value of the radial velocity, $v_{\rm r} = -10.30 \pm 0.05 \, {\rm km \, s^{-1}}$, is consistent with the value given in the Pulkovo compilation (Gontcharov 2006), $v_{\rm r} = -12.2 \pm 2.4 \, {\rm km \, s^{-1}}$.

4.3. TIC 93522454 (HD 143487)

The presence of resolved magnetically split lines in the spectrum of HD 143487 was first reported by Freyhammer et al. (2008). Here we analyse the FEROS spectrum and the UVES spectrum that they obtained in 2007, two UVES spectra from 2008 and one from 2010, and a HARPS spectrum from 2011, in addition to a recent (2023) SALT-HRS spectrum that we recorded as part of the present project.

The blend affecting the blue side of the Fe II λ 6149.2 Å line is exceptionally strong: at some epochs, it is deeper than the

Fe line itself, in contrast to its appearance in the vast majority of Ap stars in which the latter is resolved (see Figs. 2 to 4 of Mathys et al. 1997). This makes the determination of the mean magnetic field modulus from the splitting of Fe II λ6149.2 Å particularly difficult. Unfortunately, due to the very high line density in the spectrum of HD 143487, we could not identify any other Fe line with a pure doublet or triplet Zeeman pattern that could be used to derive the value of $\langle B \rangle$ in a similar approximation-free manner. As a result, the estimated uncertainties of the reported values of this magnetic field moment are considerably higher than in most other studied stars. However, the seven measurements that we obtained, which range from $\langle B \rangle = 4.00 \pm 0.10 \,\mathrm{kG}$ to $\langle B \rangle = 4.47 \pm 0.10 \,\mathrm{kG}$, appear reasonably consistent with each other, with possibly some indication of actual variability (see below). The values from the first two epochs do not significantly differ from those reported by Freyhammer et al. (2008). The value of the mean magnetic field modulus that we determine from the UVES spectrum of JD 2 455 374, $\langle B \rangle = 4.20 \pm 0.06$ kG, differs from that reported by Kochukhov et al. (2013), $\langle B \rangle = 4.75 \,\mathrm{kG}$. However, the latter was derived from the consideration of lines of rare earth elements, so that it is not directly comparable to our measurement based on an Fe line. This is especially true given the presence of chemical inhomogeneities on the surface of HD 143487, indicated by line intensity variability (see below). The distribution of Fe and of the rare earth elements is likely different, so that their lines do not sample the magnetic field in the same way.

Because of the high line density, the number of Fe I lines that could be used to diagnose the mean quadratic magnetic field is much smaller than usual, even though more severe blending was accepted in the line selection. The challenge of finding suitable diagnostic lines was compounded by the rather low S/N of most of the spectra. In addition, for UVES, only lines with wavelengths $\lambda \gtrsim 4900 \,\text{Å}$ are within the spectral range covered with the configuration selected for the observation. However, the availability of four spectra obtained at different epochs with this instrument allowed us to use the same approach as had been adopted in M24 for TIC 167695608 to untangle more efficiently the contributions of the various broadening terms to the observed line widths. Namely, we assumed that the intrinsic and Dopplerlike broadening terms do not vary with rotation phase to average them over the four epochs, and only determined the magnetic broadening term at each individual epoch, allowing better precision to be achieved in the derived values of $\langle B_{\rm q} \rangle$ (see Sect. 3.2.2 of M24 for details).

Formally significant $\langle B_q \rangle$ values could be obtained from three of the four UVES spectra and from the FEROS and SALT-HRS spectra. The value obtained with HARPS is below the level of formal significance, and the value derived from the fourth UVES spectrum marginally below this level. This must, at least in part, be due to the comparatively low S/N of the HARPS spectrum, to the limited number of suitable diagnostic lines, and to the fact that many of them suffer an amount of blending greater than in the other stars considered in this work. Given the evidence for super-slow rotation of HD 143487, the upper limits of the projected equatorial velocity derived from analysis of the various spectra, between $v \sin i \lesssim 5.8 \,\mathrm{km \, s^{-1}}$ and $v \sin i \lesssim 7.5 \,\mathrm{km \, s^{-1}}$, strongly suggest the occurrence of significant crosstalk between the magnetic and Doppler terms of the regression analysis performed to untangle them. This interpretation if further supported by the fact that Kochukhov et al. (2013) give a value $v \sin i = 1.5 \,\mathrm{km \, s^{-1}}$ for the projected equatorial velocity. In turn, the occurrence of crosstalk probably accounts for the fact that the low values of $\langle B_q \rangle$ determined in all cases

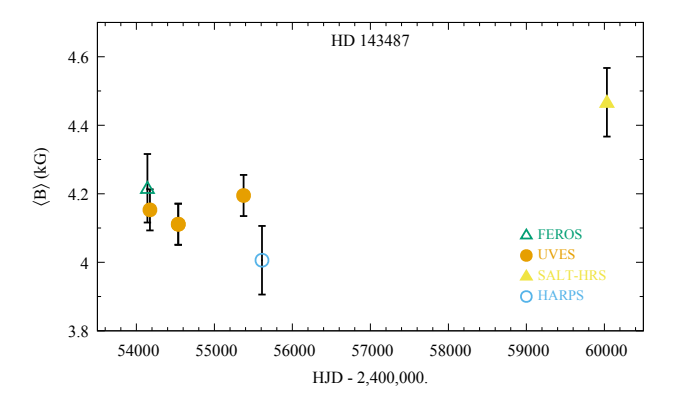


Fig. 2. Mean magnetic field modulus of HD 143487 against observation date. Different point types and colours are used to distinguish the observations performed with different instruments.

are only at most marginally consistent with the $\langle B \rangle$ values. Most likely, these $\langle B_0 \rangle$ values are underestimated because of crosstalk.

While HD 143487 was not identified as an ssrAp star candidate in our TESS-based survey, probably because of instrumental noise, Holdsworth et al. (2021) report the absence of rotational signal in their analysis of the TESS data for this star. The spectra obtained at different epochs, illustrated in Fig. A.5, suggest that the intensities of lines of some ions vary over time scales of years. The mean magnetic field modulus, despite the unusually large uncertainty affecting its measured values, may also be showing an actual long-term trend, with a minimum possibly occurring around 2011–2012 (JD~2,456,000.) or somewhat later (see Fig. 2).

The wavelength calibration of the FEROS spectrum of HD 143487 is inadequate to determine the radial velocity. The radial velocity values derived from the observations obtained with the other instruments at the six other epochs range from $v_r = -25.2 \pm 1.0 \, \mathrm{km \, s^{-1}}$ to $v_r = -14.0 \pm 0.8 \, \mathrm{km \, s^{-1}}$. The variability that they reflect is consistent with the fact that HD 143487 is a spectroscopic binary with an orbital period $P_{\mathrm{orb}} = 1353^{\mathrm{d}}9 \, \mathrm{d}$ whose centre of mass has a radial velocity $v_r = -23.97 \, \mathrm{km \, s^{-1}}$ (Gaia Collaboration 2023).

HD 143487 is a known roAp star. Elkin et al. (2010) discovered low amplitude pulsations in radial velocity variations in an ensemble of spectral lines with a period around 10 min. Kochukhov et al. (2013) obtained a time-resolved series of 62 spectra over 1.4 h with UVES and directly detected radial velocity variations in lines of Nd III and Pr III, and in the core of H α , with a period of 9.63 min. There is only one Sector of TESS data, S12, where the highest peak in the amplitude spectrum has a frequency consistent with the frequency of the radial velocity variations, although the significance of that peak is marginal (Holdsworth et al. 2021).

4.4. TIC 163801263 (HD 203922)

A spectrum of HD 203922 obtained with the Catania Astrophysical Observatory Spectropolarimeter (CAOS; Leone et al. 2016) was analysed in M24. Both the mean magnetic field modulus and the mean quadratic magnetic field could be determined. The magnetically split components of the $\langle B \rangle$ diagnostic line, Fe II λ 6149.2 Å, which were only marginally resolved in the CAOS spectrum, are now fully resolved with HARPS-N, so that a much more precise value of the mean field modulus can be derived here, $\langle B \rangle = 3503 \pm 30\,\mathrm{G}$. The value of the quadratic

field measurement, $\langle B_q \rangle = 3830 \pm 120\,\mathrm{G}$ has a formal uncertainty among the lowest achieved as part of this project. Within the uncertainties, neither the mean magnetic field modulus nor the mean quadratic magnetic field show any significant change between the epochs of the CAOS and HARPS-N observations, which are almost 2 years apart. This lends plausibility to a very long rotation period, of the order of several years. However, the upper limit derived here for the projected equatorial velocity, $v \sin i \lesssim 3.7\,\mathrm{km\,s^{-1}}$, while more stringent than the value $v \sin i \lesssim 5.3\,\mathrm{km\,s^{-1}}$ of M24, does not rule out a moderately long rotation period.

The radial velocity does not show any significant change either between the two epochs of observation. The formal uncertainty achieved in its determination from the HARPS-N spectrum, 0.05 km s⁻¹, is among the lowest obtained within the framework of this project.

4.5. TIC 170419024 (HD 151860)

Here we complement the results from M24 on HD 151860 by the analysis of the UVES spectrum of 2010 that was part of the study of Kochukhov et al. (2013). The value of the mean magnetic field modulus derived by measuring the splitting of the Fe II λ 6149.2 Å line in this spectrum, $\langle B \rangle = 2265 \pm 40 \,\text{G}$, is considerably smaller than the value determined in the 2023 SALT-HRS spectrum of M24, $\langle B \rangle = 3356 \pm 100 \,\text{G}$. This confirms the conclusion that the relative amplitude of variation of the magnetic field of HD 151860 is above average, inferred from consideration of the change in the mean quadratic magnetic field between a FEROS spectrum from 2008 and a SALT-HRS spectrum of 2023. The value from 2010 obtained here, $\langle B_q \rangle = 2.58 \pm 0.17 \,\text{kG}$ does not significantly differ from the 2008 value, $\langle B_{\rm q} \rangle = 2.51 \pm 0.28 \, \text{kG}$, but both are much lower than the 2023 value, $\langle B_q \rangle = 5.41 \pm 0.56$ kG. The mean quadratic field may plausibly have been varying monotonically from 2008 to 2023, which would indicate a rotation period of the order of 25 years or more.

However, this conjecture needs to be confirmed by additional observations, especially since the value of the projected equatorial velocity derived by Kochukhov et al. (2013), $v \sin i = 4.5 \, \mathrm{km \, s^{-1}}$, which is reasonably consistent with the upper limit that we determine here, $v \sin i \leq 4.2 \pm 0.3 \, \mathrm{km \, s^{-1}}$, seems somewhat large for a period of decades. (The magnetic field strength of 2.5 kG that Kochukhov et al. infer from spectrum synthesis analysis is also compatible with our determinations of $\langle B \rangle$ and $\langle B_{\rm q} \rangle$.)

The difference between the values of the radial velocity measured from the 2010 UVES spectrum ($v_{\rm r}=3.45\pm0.07\,{\rm km\,s^{-1}}$) and the 2023 SALT-HRS spectrum ($v_{\rm r}=4.10\pm0.25\,{\rm km\,s^{-1}}$) is marginal. Both values are also consistent with the one from the Gaia DR2 (Gaia Collaboration 2018) ($v_{\rm r}=3.67\pm0.39\,{\rm km\,s^{-1}}$). Thus there is no clear evidence of binarity for HD 151860, contrary to what was mistakenly reported in M24 (see Mathys et al. 2025).

4.6. TIC 238659021 (HD 8441)

Babcock (1958) discovered the magnetic field of the well studied Ap star HD 8441 and obtained a series of measurements of its mean longitudinal component ranging from -750 to +400 G. However, the most precise determinations of this field moment to date, achieved by Aurière et al. (2007), yielded a maximum absolute value $|\langle B_z \rangle|_{\rm max} = 157 \pm 18$ G. This value is consistent with the fact that the mean quadratic magnetic field is below the

detection limit in our analysis of a HARPS-N spectrum (using Fe II diagnostic lines). Visual inspection of our HARPS-N spectrum does not show any evidence of differential line broadening, contrary to the case of BD+35 5094 (Sect. 4.10). Based on this result, by comparison with other stars of this study, we estimate that $\langle B_q \rangle$ must definitely be lower than 1 kG, which is inconsistent with mean longitudinal field values significantly greater than 200–300 G. The uncertainties of the measurements of HD 8441 reported by Babcock (1958) must have been underestimated. Titarenko et al. (2012) also mention the absence of any magnetic enhancement of the spectral lines, lending further support to the conclusion that, while HD 8441 is definitely a magnetic Ap star, it has one of the weakest fields in the class.

The upper limit of the projected equatorial velocity that we derive from our analysis, $v \sin i \lesssim 3.1 \pm 0.2 \, \mathrm{km \, s^{-1}}$, is consistent with the published value $v \sin i \leq 2.9 \pm 0.6 \, \mathrm{km \, s^{-1}}$ (Carrier et al. 2002). The rotation period of this ssrAp star, $P_{\rm rot} = 69^{.4}51 \pm 0^{.4}01$, is well determined (Pyper & Adelman 2017). Using the radius value from the TIC ($R = 5.16 \, \mathrm{R}_{\odot}$), and $P_{\rm rot} = 69^{.4}51 \pm 0^{.4}01$, we find an equatorial rotation velocity of $v_{\rm eq} = 2\pi R/P = 3.76 \, \mathrm{km \, s^{-1}}$. Coupled with our determination of $v \sin i \lesssim 3.1 \pm 0.2 \, \mathrm{km \, s^{-1}}$, this yields $i \lesssim 56^{\circ}$. This limit is not very stringent.

North et al. (1998) determined the orbital parameters of the 'short' period ($P_{\text{orb}} = 106\rlap.^d.357$) within the HD 8441 triple system. The epoch of our HARPS-N observation corresponds to orbital phase 0.937 ± 0.008 . The value that we derive for the radial velocity, $v_r = 3.68 \pm 0.03 \, \text{km s}^{-1}$, appears consistent with the curve shown in Fig. 1 of North et al.

4.7. TIC 251976407 (HD 221568)

Preston (1971) determined a magnetic field strength of 1.8 kG from the analysis of differential magnetic broadening of spectral lines with narrow and broad Zeeman patterns in HD 221568. The value that he derived has essentially the same physical meaning as the mean quadratic magnetic field. In the spectrum that he analysed, the lines were not resolved into their magnetically split components.

By contrast, in our HARPS-N spectrum of HD 221568, the two components of the Fe II λ 6149.2 Å line are resolved. The unidentified blending line on the blue side of Fe II λ6149.2 Å is separated enough from the latter so that good precision is achievable in the determination of the mean magnetic field modulus, $\langle B \rangle = 2433 \pm 30 \,\mathrm{G}$. Although the uncertainty of the field value obtained by Preston is unknown, the difference between it and the value of that we derive for the mean quadratic magnetic field, $\langle B_q \rangle = 2790 \pm 250 \,\mathrm{G}$, is probably significant and representative of the actual variability of the observed field as a result of stellar rotation. Unfortunately, we do not know the date on which the data analysed by Preston were obtained, so that we cannot estimate the phase difference between the two measurements, even though the accuracy of the value of the rotation period, $P_{\text{rot}} = 159.10 \pm 0.03$ (Pyper & Adelman 2017), is good enough to derive a meaningful constraint. The occurrence of $\langle B_{\rm q} \rangle$ variations of rather large amplitude appears especially plausible considering the variability of the spectral line intensities (summarised by Pyper & Adelman) and the significant difference between the values of the mean longitudinal magnetic field determined at two epochs separated by 19 d Romanyuk et al. (2018): $\langle B_z \rangle = 722 \pm 32 \,\text{G} \text{ and } \langle B_z \rangle = 461 \pm 34 \,\text{G}.$

Contrary to other stars for which the published value of the effective temperature is similar, such as HD 89069 (Sect. 4.9), the lines of Fe I in HD 221568 are weak or absent, so that the

diagnostic lines used for the present analysis pertain to Fe II. Their rotational broadening is below the detection limit, which is consistent with the long rotation period. The radial velocity value at the epoch of our observation, $v_r = -8.33 \pm 0.12 \,\mathrm{km \, s^{-1}}$, differs significantly from those published by Romanyuk et al. (2018): $-6.9 \pm 2.7 \,\mathrm{km \, s^{-1}}$ and $-0.3 \pm 2.4 \,\mathrm{km \, s^{-1}}$. Thus, HD 221568 appears to be a spectroscopic binary.

4.8. TIC 301918605 (HD 17330)

The mean quadratic magnetic field of HD 17330 was below the detection threshold in our previous analysis of a CAOS spectrum (M24). Here, based on a HARPS-N spectrum, we achieve a 6.3 σ determination of the value of this field moment, $\langle B_{\rm q} \rangle = 1130 \pm 180\,\rm G$. We also derive a much more stringent upper limit of the projected equatorial velocity, $v \sin i \lesssim 1.4 \pm 0.1\,\rm km\,s^{-1}$, which confirms that HD 17330 must be an ssrAp star. The value of the radial velocity, $v_{\rm r} = -12.42 \pm 0.03\,\rm km\,s^{-1}$, is the most precise one measured as part of this study. While small, the difference between it and the value obtained from the CAOS spectrum recorded 806 d earlier, $v_{\rm r} = -13.10 \pm 0.12\,\rm km\,s^{-1}$, is significant, consistent with reports in the literature that HD 17330 is a spectroscopic binary (M24).

4.9. TIC 341616734 (HD 89069)

Romanyuk et al. (2020) discovered the magnetic field of HD 89069. Their four measurements of the mean longitudinal magnetic field (see also Romanyuk et al. 2017) range from $\langle B_z \rangle = -720\,\mathrm{G}$ to $\langle B_z \rangle = 20\,\mathrm{G}$, indicating variability on a time scale of days to weeks. Analysis of two HARPS-N spectra of the star yield determinations of the mean quadratic magnetic field at the ~29 σ and ~36 σ level. The precision of the latter measurement, 90 G, is the best we have ever achieved for any star. It appears to represent the precision limit achievable with the observations that we are performing. However, the derived value of $\langle B_q \rangle$ does not show any significant change between the two epochs of observation, 23 d apart.

Despite the relatively high derived value, $\langle B_q \rangle \simeq 3.3$ kG, the spectral lines observed in the visible spectrum of HD 89069 are not resolved into their magnetically split components at the epoch of our observation, even though some of them (for instance, Fe II λ 6149.2 Å and Fe I λ 6336.8 Å) show clear magnetic broadening. This reflects the fact that magnetic resolution is smeared out by a moderate amount of rotational broadening, consistent with the upper limit of the projected equatorial velocity derived from our analysis, $v \sin i \lesssim 4.3$ km s⁻¹. Nevertheless, one should keep in mind that depending on magnetic variability, which cannot be characterised yet, some spectral lines (for instance, Fe II λ 6149.2 Å) may show at least partial magnetic resolution over part of the stellar rotation cycle.

Burke & Lady (1977) reported that HD 89069 is photometrically variable. The time range spanned by their observations was too short to determine the rotation period, but they showed an illustration based on an assumed, arbitrary value $P_{\text{rot}} = 18 \text{ d}$. The TESS data show no evidence of such a period (Mathys et al. 2022).

The star was mistakenly labelled as HD 86069 in Fig. B.6 of Mathys et al. (2022). There are now 120-s TESS data available for Sectors 14, 20, 21, 26, 40, 41, 47, and 53, with the earlier data reprocessed. An amplitude spectrum of the data ensemble shows a hump of low-frequency amplitude, but no obvious α^2 CVn rotational peak. The amplitude spectrum out to a frequency 5 d⁻¹ does not look significantly different from

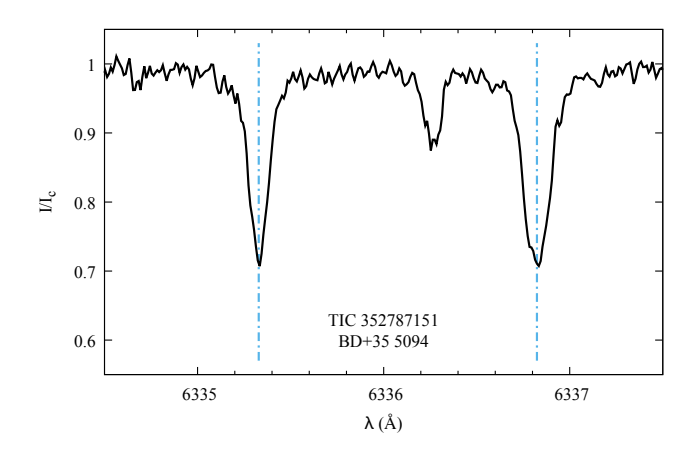


Fig. 3. Comparison of the profiles of the Fe I λ 6335.3 Å and λ 6336.8 Å lines in BD+35 5094. The wavelengths are in the laboratory reference frame. The Zeeman patterns of the lines seen in the considered wavelength range were shown in Fig. 6 of M24. One can clearly see that Fe I λ 6336.8 Å is significantly broader than Fe I λ 6335.3 Å, which reveals the presence of a magnetic field in BD+35 5094.

Fig. B.6 of Mathys et al. (2022). Despite the reported variability of the mean longitudinal magnetic field, no rotational modulation is apparent in the TESS photometric data. Nevertheless, the reported magnetic variability and the probable rotational broadening of the spectral lines (see above) suggest that HD 89069 is more likely a star with a moderately long period ($20 \, \text{d} \lesssim P_{\text{rot}} \lesssim 50 \, \text{d}$) than an ssrAp star.

The measurements of Romanyuk et al. (2017) and Romanyuk et al. (2020) suggest that the radial velocity of HD 89069 is variable, albeit close to the threshold of significance, given the rather large uncertainties (up to $4.4\,\mathrm{km\,s^{-1}}$) of the derived values. Our determinations, $v_{\rm r} = -9.23 \pm 0.10\,\mathrm{km\,s^{-1}}$ and $v_{\rm r} = -9.17 \pm 0.05\,\mathrm{km\,s^{-1}}$ are within the range spanned by the published ones ($-12.7\,\mathrm{km\,s^{-1}} \lesssim v_{\rm r} \lesssim 3.8\,\mathrm{km\,s^{-1}}$), but they do not significantly differ from each other. The binarity of HD 89069 needs to be confirmed by additional precise radial velocity measurements.

4.10. TIC 352787151 (BD+35 5094)

The mean quadratic field of BD+35 5094 was below the detection limit in our analysis of a CAOS spectrum reported in M24. We suspected the occurrence of some crosstalk between the rotation and magnetic terms of the regression carried out to untangle the various broadening contributions to the observed line width. This suspicion was borne out by the rather high value derived for the upper limit of the projected equatorial velocity $(v \sin i \le 6.8 \pm 0.6 \, \mathrm{km \, s^{-1}})$. Its plausibility is strengthened by the fact that we determine here a much lower value of this upper limit, $v \sin i \le 2.0 \pm 0.2 \, \mathrm{km \, s^{-1}}$, from the analysis of a HARPS-N spectrum. In the latter, there does not appear to be any significant crosstalk between the rotation and magnetic terms. Accordingly, it is rather unexpected that the mean quadratic magnetic field remains below the detection threshold.

This is all the more surprising since the differential broadening in pairs of lines of different magnetic sensitivities is clearly seen by visual inspection of the spectrum. This is illustrated in Fig. 3, where the additional broadening of the Fe I $\lambda 6336.8\,\text{Å}$ line with respect to the neighbouring Fe I $\lambda 6335.3\,\text{Å}$ line is clearly visible. (This effect was already reported in M24.) The

former line is one of the most magnetically sensitive Fe I lines in the observed spectral range; the magnetic sensitivity of the latter is much lower (see M24 for more details). Because the two lines occur at neighbouring wavelengths and because their equivalent widths are similar, the difference between their widths can be unambiguously attributed to magnetic broadening, albeit caused by a rather weak field. The weakness of this field accounts for the failure to untangle its contribution from the intrinsic and rotational terms in the regression analysis carried out to try to determine its mean quadratic value. Based on consideration of the results of the analysis of the stars of the sample for which the lowest formally significant values of $\langle B_q \rangle$ are derived, we estimate that the mean quadratic magnetic field of BD+35 5094 must be slightly weaker than ~1 kG. Actually, the main contribution to the observed line width is the intrinsic term. With the small rotational broadening (see above), BD+35 5094 must be a weakly magnetic ssrAp star.

The value of the radial velocity derived from the HARPS-N spectrum, $v_r = -6.81 \pm 0.05 \text{ km s}^{-1}$, differs significantly from that determined from the CAOS observation obtained 2.2 yr earlier, $v_r = -9.44 \pm 0.12 \text{ km s}^{-1}$. Both values are also different from the one published in the Gaia DR2 Catalogue (Gaia Collaboration 2018), $v_r = -4.05 \pm 0.25 \text{ km s}^{-1}$. The ssrAp star BD+35 5094 belongs to a spectroscopic binary system.

4.11. TIC 356088697 (HD 76460)

The resolution of the magnetically split components of the Fe II λ6149.2 Å line in HD 76460 was first reported by Elkin et al. (2012), who derived a value $\langle B \rangle = 3.6 \pm 0.2 \,\mathrm{kG}$, based on a FEROS spectrum recorded in 2010 January. We analysed this spectrum, as well as a SALT-HRS spectrum obtained in 2023 April. The value of the mean magnetic field modulus that we determined from the latter, $\langle B \rangle = 3607 \pm 40 \,\mathrm{G}$, is not significantly different from that of Elkin et al. (2012). The latter is also fully consistent with the value that we derive by application of our measurement procedure to a SALT-HRS spectrum: $\langle B \rangle = 3586 \pm 50 \,\text{G}$. The low estimated uncertainty of our determinations reflects the absence of any major blending of the Fe II λ 6149.2 Å line, so that the measurement of its splitting is straightforward. The fact that the mean magnetic field modulus does not appear to have changed between two epochs of observation separated by more than 13 years suggests that the rotation period of HD 76460 may be extremely long. This view is consistent with its identification as an ssrAp star candidate (Mathys et al. 2020), as well as with the values determined for the upper limit of the projected equatorial velocity.

Indeed, Elkin et al. (2012) found $v \sin i \lesssim 3.0 \,\mathrm{km \, s^{-1}}$. As part of the analysis of the spectra for determination of the mean quadratic magnetic field, we derived $v \sin i \leq 4.0 \,\mathrm{km \, s^{-1}}$ (FEROS) and $v \sin i \lesssim 3.9 \,\mathrm{km \, s^{-1}}$ (SALT-HRS). The values of the mean quadratic magnetic field determined at the two epochs, $\langle B_{\rm q} \rangle = 3890 \pm 260 \,\text{G} \,(2010) \,\text{and} \,\langle B_{\rm q} \rangle = 3350 \pm 340 \,\text{G} \,(2023), \,\text{are}$ consistent with each other within the uncertainties. If any variation has occurred over the elapsed ~13 yr, it appears moderate. This lends additional plausibility to the view that HD 76460 may have a rotation period of the order of decades. Both derived values of the mean quadratic magnetic field are low with respect to the mean field modulus, but not inconsistent with it. However, this raises some concerns about the possible occurrence of crosstalk between the magnetic, Doppler and intrinsic contributions in the multi-dimensional least-squares fit of the observed second-order moments of the Stokes I line profiles about their centres (see Sect. 3.2.1 of M24). Nevertheless, critical evaluation of the analysis procedure does not show any clear indication of such crosstalk. An intriguing possible alternative interpretation is that HD 76460 has an unusual magnetic field structure. It would be interesting to obtain spectropolarimetric observations to gain further insight into this possibility.

The wavelength calibration of the FEROS spectrum is inadequate for determination of the radial velocity. Accordingly, we cannot assess the possible binarity of HD 76460.

4.12. TIC 369969602 (HD 128472)

Very little is known about HD 128472, which appears to be studied in some detail for the first time here. We detected its magnetic field from analysis of a SALT-HRS spectrum: $\langle B_q \rangle = 1840 \pm$ 570 G. At the 3.2 σ level, this value is just above the threshold of formal significance, but critical inspection of the dependences of the various broadening contributions to the line profile width does not suggest any significant crosstalk between them, so that the detection can be regarded as firm. This is also supported by visual inspection of the Fe II $\lambda 6335.3 \,\text{Å}$ and $\lambda 6336.8 \,\text{Å}$ lines, as the latter appears marginally broader than the former. On the other hand, the upper limit of the projected equatorial velocity derived as part of the same analysis, $v \sin i \lesssim 3.3 \,\mathrm{km \, s^{-1}}$, is consistent with super-slow rotation, but a moderately long rotation period (20 d $\lesssim P_{\rm rot} \lesssim 50$ d) cannot be definitely ruled out. Our single measurement of the radial velocity of HD 128742 cannot be used to assess its binarity since no other determination could be found in the literature.

4.13. TIC 380607580 (HD 119794)

The SALT-HRS spectrum of HD 119794 shows resolved magnetically split lines. The Fe II λ6149.2 Å line suffers only minimal blending, so that the estimated uncertainty on the derived value of the mean magnetic field modulus is low: $\langle B \rangle = 5369 \pm$ 40 G. We used Fe II diagnostic lines to determine the mean quadratic magnetic field, $\langle B_q \rangle = 4800 \pm 400$ G. This value is low compared to that of the mean field modulus. One may suspect that the value of $\langle B_q \rangle$ is underestimated because of the occurrence of crosstalk between the three terms contributing to the line broadening in the regression analysis carried out to untangle them (see M24 for details). There is no unambiguous indication of such crosstalk in the present case, but the upper limit derived for the projected equatorial velocity, $v \sin i \lesssim 6.1 \pm 0.5 \,\mathrm{km \, s^{-1}}$, seems somewhat high given the appearance of the magnetically split components of the Fe II λ 6149.2 Å line. On the other hand, the Fe diagnostic lines in HD 119794 are stronger than in most other stars analysed in this work. Accordingly, the weak line approximation underlying the method of determination of the mean quadratic magnetic field (Mathys & Hubrig 2006) may be less justified than in other cases. This may plausibly lead to underestimating the value of $\langle B_q \rangle$.

Regardless, HD 119794 is definitely an Ap star with a sizeable magnetic field that either rotates extremely slowly or must have a moderately long rotation period. We could not find any published value of its radial velocity in the literature, and hence we could not assess its binarity from our single measurement.

4.14. TIC 403625657 (HD 11187)

The conclusion that 'HD 11187 is definitely a magnetic Ap star that does not rotate particularly slowly', based on the analysis of a CAOS spectrum (M24), was reached only shortly before the

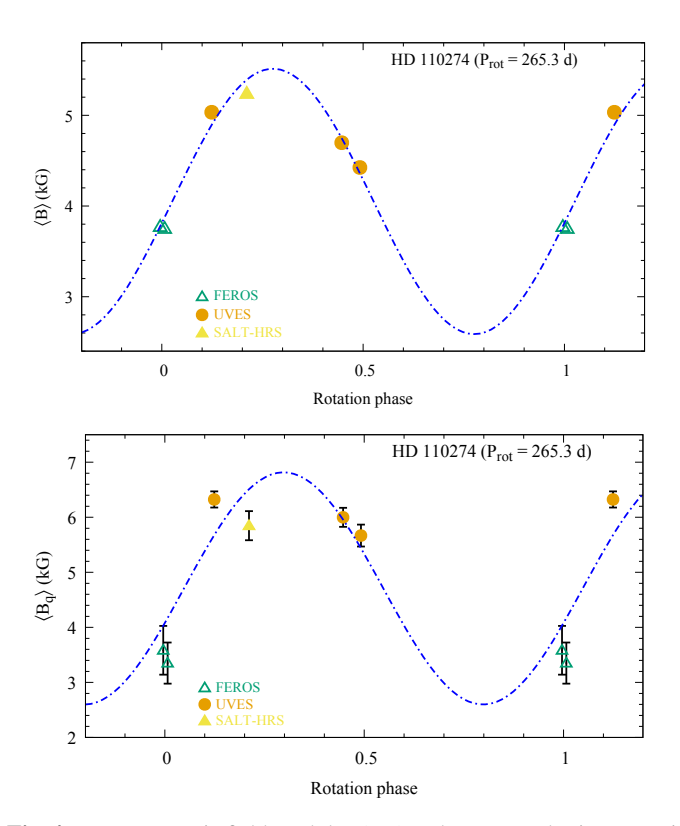


Fig. 4. Mean magnetic field modulus (*top*) and mean quadratic magnetic field (*bottom*) of HD 110274 against rotation phase computed with the value $P_{\rm rot} = 265^{\rm d}3$ of the rotation period derived by Freyhammer et al. (2008). The phase origin has been set at JD 2454140.0. The dash-dotted blue curve represents the least-squares fit of the measurements by a sine curve. Different point types and colours are used to distinguish the observations performed with different instruments. The size of the error bars for the $\langle B \rangle$ values does not exceed that of the symbols representing them.

star was re-observed with HARPS-N. Despite the higher resolution and S/N of this latter spectrum, the mean quadratic magnetic field remains below the detection threshold. The line broadening is largely dominated by the rotational Doppler effect. The upper limit of the projected equatorial velocity that we derived from analysis of the HARPS-N spectrum, $v \sin i \le 15.3 \pm 0.1 \, \mathrm{km \, s^{-1}}$, is at most marginally lower than the CAOS-based value, $v \sin i \le 17.7 \pm 0.8 \, \mathrm{km \, s^{-1}}$. It remains compatible with a rotation period of the order of days to weeks, as indicated by the variability of the mean longitudinal magnetic field reported by the group of the Special Astrophysical Observatory (Romanyuk, private communication).

The values of the radial velocity determined from the CAOS $(v_r = 5.61 \pm 0.27 \,\mathrm{km\,s^{-1}})$ and HARPS-N $(v_r = 5.73 \pm 0.06 \,\mathrm{km\,s^{-1}})$ spectra, obtained almost 2 yr apart, do not significantly differ from each other. There is no indication of binarity for HD 11187.

4.15. TIC 405516045 (HD 110274)

Freyhammer et al. (2008) discovered resolved magnetically split lines in the spectrum of HD 110274. Their analysis was based on two FEROS spectra and one UVES spectrum obtained at different epochs in 2007. The same group acquired UVES observations at two epochs in 2008, which have not been used until now for magnetic field diagnosis. We added a sixth epoch with a SALT-HRS spectrum recorded in 2023.

We performed determinations of the mean magnetic field modulus and of the mean quadratic magnetic field from all six spectra. The values of $\langle B \rangle$ that we derived from the FEROS spectra are fully consistent with those reported by Freyhammer et al. (2008). However, our analysis of the 2007 UVES spectrum yielded $\langle B \rangle = 5.25 \,\mathrm{kG}$, which is significantly greater than the value $\langle B \rangle = 4.45 \,\mathrm{kG}$ published by Freyhammer et al. from a measurement of the same Fe II λ6149.2 Å diagnostic line. We do not understand the origin of this discrepancy, especially considering that the measurement is quite straightforward as the Fe II λ6149.2 Å line in HD 110274 suffers only minor blending of its blue component by the unidentified line that severely affects it in other Ap stars. Comparison of the line splitting with that observed at other epochs strengthens our conviction that the value of $\langle B \rangle$ that we derive from the UVES observation of 2007 is correct and precise.

The values of $\langle B \rangle$ and $\langle B_{\rm q} \rangle$ are plotted in Fig. 4 against the rotation phase computed using the value of the period, $P_{\rm rot}=265^{\rm d.3}$, derived from photometric observations by Freyhammer et al. (2008). Both magnetic field moments show variability with a relative amplitude above average. They appear to vary nearly in phase with each other, which is not unusual. (For comparison, see Mathys 2017.) However, the phase coverage of the measurements obtained until now is very incomplete, with a phase gap of more than 0.5 cycle around the $\langle B \rangle$ and $\langle B_{\rm q} \rangle$ minima. Accordingly, the sine curve that is fitted to the data is only indicative; the actual shape of the variation could significantly depart from it. Observations at more epochs are needed to settle this issue.

For two of the UVES spectra, the Doppler contribution to the line broadening is below the detection threshold. This is fully consistent with the length of the rotation period, $P_{\text{rot}} = 265^{\text{d}}$ 3.

Finally, we discovered significant variations of the radial velocity of HD 110274. The wavelength calibration of the first epoch FEROS spectrum is inadequate for radial velocity determination. The values determined at the five remaining epochs of observation range from $v_{\rm r} = -7.75 \pm 0.08 \, {\rm km \, s^{-1}}$ to $v_{\rm r} = -1.43 \pm 0.10 \, {\rm km \, s^{-1}}$. This ssrAp star HD 110274 definitely belongs to a spectroscopic binary, but the number of observations is insufficient to constrain the orbital period.

4.16. TIC 419916333 (HD 117290)

The presence of resolved magnetically split lines in the spectrum of HD 117290 was first reported by Freyhammer et al. (2008). The values of the mean magnetic field modulus that they derived from measurement of two FEROS spectra and one UVES spectrum spanning one month in 2007 do not show any significant variation. We reanalysed these spectra together with another UVES observation (from 2008) from the ESO Archive and a SALT-HRS spectrum that we recorded in 2023. The Fe II λ 6149.2 Å line is almost free from blends, so that the $\langle B \rangle$ values can be precisely determined. Those that we derived from the 2007 spectra average at 6360 G, consistent with the result published by Freyhammer et al. (2008). The more recent spectra yield very different values: $\langle B \rangle = 4509 \pm 30\,\mathrm{G}$, in 2008, and $\langle B \rangle = 3020 \pm 40\,\mathrm{G}$, in 2023.

The ratio between the highest and lowest measured values of the mean magnetic field modulus, $q \sim 2.1$, is exceptionally large. Among the Ap stars for which this value has been determined until now, it is exceeded only by HD 9996 ($q \sim 3.3$, Giarrusso et al. 2022) and HD 57372 ($q \sim 3$, Hubrig et al. 2024), and of the same order as HD 29578 ($q \sim 2.0$, Giarrusso et al. 2022) and HD 65339 ($q \sim 1.95$, Mathys 2017). This makes it

probable that the 2007 spectra were recorded in a phase interval around the $\langle B \rangle$ maximum and the 2023 spectrum in the vicinity of the phase of its minimum. If this speculation is correct, the $\sim 16 \, \mathrm{yr}$ elapsed before the first and the most recent observations considered here must approximately correspond to an odd number of half rotation cycles.

We did not identify HD 117290 as an ssrAp star candidate as part of our TESS-based systematic survey. However, a lower limit of the rotation period, $P_{\text{rot}} \gtrsim 5.7 \,\text{yr}$, had been derived from photometry by Freyhammer et al. (2008). Taking this into account, the star may not have completed much more than 2.5 rotation cycles in 16 yr. On the other hand, the change undergone by the mean magnetic field modulus from 2007 to 2008, ~1.8 kG, is close to half the difference between the highest and lowest measured $\langle B \rangle$ value, which does not appear compatible with a rotation period much longer than 5.7 yr. Simultaneous consideration of these two constraints suggests that the rotation period of HD 117290 must be of the order of 6 yr. Admittedly, this conclusion relies on educated guesses that are not proven, but it suggests that scheduling future observations so as to test the viability of a ~6 yr period represents the strategy with the highest chances of success.

The line density is very high in the spectrum of HD 117290, which limits the number of Fe I lines that can be selected to diagnose the mean quadratic magnetic field, even relaxing the blend-free requirement applied to most other stars of this study. Furthermore, the star undergoes considerable spectral line intensity variations along its rotation cycle, so that different sets of diagnostic lines must be used at different phases. The variability is illustrated in Fig. A.6, which shows the same spectral range as Figs. A.1 to A.3 as observed at different epochs and with different instruments in HD 117290. In this range, variability is observed mainly in the lines of Cr, Nd and Pr, which all appear stronger when the magnetic field is weaker. In other wavelength regions, identification of the variable lines is not straightforward and requires detailed analysis that is beyond the scope of the present work.

Similar to the mean magnetic field modulus, and apparently in phase with it, the mean quadratic magnetic field shows variations of large amplitude. The derived values of the two field moments are mostly consistent with each other, albeit only marginally so in 2023, when $\langle B_{\rm q} \rangle < \langle B \rangle$. This formal discrepancy is well within the error margin, but may in part at least result from the occurrence of a small amount of crosstalk between the rotational and magnetic contributions to the line broadening. The latter might also explain why a formally significant upper limit of the projected equatorial velocity, $v \sin i \lesssim 2.3 \pm 0.6 \, {\rm km \, s^{-1}}$ is derived (which is compatible with a rotation period of years) while rotational broadening is below the detection limit in the other analysed spectra.

Finally, radial velocity variations, indicative of binarity, are definitely detected. The wavelength calibration of the first-epoch FEROS spectrum is inadequate for radial velocity determination, but the values derived for the later four epochs range from $v_r = -36.97 \pm 0.20 \, \mathrm{km \, s^{-1}}$ to $v_r = -4.47 \pm 0.15 \, \mathrm{km \, s^{-1}}$. The fact that the two values measured one month apart in 2007 hardly differ from each other makes a long orbital period (of the order of years) plausible, but this is not conclusive. Further observations are required to obtain more meaningful constraints.

TESS photometry shows a rich δ Sct frequency spectrum, which is unusual for an Ap star. One may suspect the pulsation signal to arise from the secondary of the binary system. As the δ Sct frequencies extend up to $40\,\mathrm{d}^{-1}$, this component is unlikely to be cooler than $T_{\mathrm{eff}} \sim 7300\,\mathrm{K}$, the value appearing

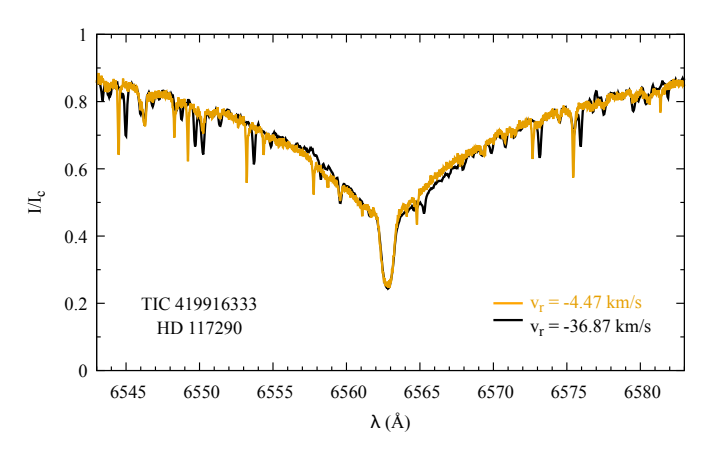


Fig. 5. Spectra of HD 117290 at the epochs of the lowest and highest radial velocity values that were recorded in this study, $v_{\rm r}=-4.47\,{\rm km\,s^{-1}}$ (2008 UVES spectrum) and $v_{\rm r}=-36.87\,{\rm km\,s^{-1}}$ (2023 SALT-HRS spectrum). If lines of the two components of the binary are visible, this is when the greatest wavelength separation between them has been observed. The laboratory reference frame was used for the wavelengths of the lines of the sharp-lined Ap component. In this reference frame, the blue wing of the H\$\alpha\$ line is less depressed in the SALT-HRS spectrum than in the UVES one, and conversely, its red wing is more depressed in the SALT-HRS spectrum than in the UVES one. This is consistent with the presence of a (very) broad H\$\alpha\$ line from the secondary that is blue shifted in 2008 and redshifted in 2023 with respect to the H\$\alpha\$ line of the Ap star, which has a much narrower core. (The pairs of very narrow lines that appear shifted with respect to each other between the two spectra are of telluric origin.)

in the TIC for HD 117290. Thus, its contribution should be visible in the observed spectrum. It is not apparent in the metal lines, probably because of rapid rotation. This interpretation is borne out by consideration of Fig. 5, in which one can distinguish a very broad $H\alpha$ profile that undergoes a wavelength shift evolving with time with respect to the sharp-cored $H\alpha$ line of the Ap star. Thus, HD 117290 is a newly discovered double-lined spectroscopic binary (SB2) system consisting of an ssrAp star and a fast-rotating δ Sct star.

4.17. TIC 430355895 (BD+52 3124)

There is very little information in the literature about BD+52 3124 besides spectral classification. In the HARPS-N spectrum of this star, the Fe II λ 6149.2 Å line is resolved into its components by the magnetic field. Their splitting indicates a value $\langle B \rangle = 4237 \pm 50\,\mathrm{G}$ for the mean magnetic field modulus. The estimated uncertainty, 50 G, reflects the presence of a moderate blend affecting the blue component.

This is one of the few stars of the sample that is hot enough so that the lines of Fe II are better suited than those of Fe I for the diagnosis of the mean quadratic magnetic field. The value of the latter, $\langle B_{\rm q} \rangle = 4920 \pm 170\,\rm G$, is fully consistent with that of the mean magnetic field modulus. The value derived for the upper limit of the projected equatorial velocity, $v \sin i \lesssim 3.2\,\rm km\,s^{-1}$, is compatible with super-slow rotation, but it does not definitely exclude a moderately long rotation period (20 d $\lesssim P_{\rm rot} \lesssim 50\,\rm d$). We did not find any published value of the radial velocity, so that we cannot assess the binarity of BD+52 3124 on the basis of our single $v_{\rm r}$ measurement.

Table 1. Properties of the studied stars.

TIC	Other ID	Dagalyad	Magnetic	Dinority	$P_{\rm rot}$						
TIC	Other ID	lines	field	Біпагіту	rot rot						
ssrAp stars											
32259138	HD 138777	X	X								
88202438	HD 192686	X	X								
93522454	HD 143487	X	X	SB1							
170419024	HD 151860	X	X								
238659021	HD 8441		X	SB1	69451						
251976407	HD 221568	X	X	SB1	159d10						
301918605	HD 17330		X	SB1							
356088697	HD 76460	X	X								
405516045	HD 110274	X	X	SB1	265d3						
419916333	HD 117290	X	X	SB2	~6 yr?						
Long period Ap stars											
163801263	HD 203922	х	х		≥25 yr?						
352787151	BD+35 5094			SB1	~ - 5						
369969602	HD 128472		X								
380607580	HD 119794	X	X								
430355895	BD+52 3124	X	X								
470837956	BD+61 2565		X	SB1							
Moderately long period Ap star											
341616734	HD 89069		x	SB1?							
Short period Ap star											
403625657	HD 11187		X								

Notes. The table is divided into four segments. The top one includes those stars for which the analysis presented in Sect. 4 indicates that they are in all probability ssrAp stars. The spectroscopic properties of the stars listed in the second segment are consistent with their having either moderately or extremely long rotation periods. The rotation period of the star from the third segment probably is moderately long $(20 \,\mathrm{d} \lesssim P_{\mathrm{rot}} \lesssim 50 \,\mathrm{d})$. The fourth segment contains the only magnetic Ap star of this study to have a rotation period of a few days. In each segment, the stars are listed in order of increasing TIC number (Col. 1); an alternative ID is given is Col. 2. The visible range spectrum of those stars for which 'x' appears in Col. 3 shows resolved magnetically split lines; the 'x' flag in Col. 4 identifies those stars for which a significant detection of the magnetic field was achieved and at least one field moment could be determined, either in this study or in the literature (see text). Column 5 indicates which stars are spectroscopic binaries, distinguishing to the extent possible the single-lined (SB1) and double-lined systems. Finally, in Col. 6, we list the value of the rotation period, when available from the literature (the references are given in the relevant sub-sections of Sect. 4) or an estimated value or lower limit derived as part of the present study.

4.18. TIC 470837956 (BD+61 2565)

The analysis of the HARPS-N spectrum of BD+61 2565 reveals the presence of a rather strong magnetic field: $\langle B_{\rm q} \rangle = 1680 \pm 140\,\rm G$, which is detected at the 12 σ level. This implies that the mean magnetic field modulus is below the threshold of resolution of the magnetically split components of the Fe II λ 6149.2 Å line, ~1.7 kG (Mathys et al. 1997). However, the differential broadening of lines of different magnetic sensitivities is clearly seen upon visual inspection. The derived value of the upper limit of the projected equatorial velocity, $v \sin i \lesssim 3.3\,\rm km\,s^{-1}$, is consistent with super-slow rotation, or possibly a moderately long rotation period (20 d $\lesssim P_{\rm rot} \lesssim 50\,\rm d$).

The radial velocity at the epoch of the HARPS-N observation, $v_{\rm r}=-17.89\pm0.06\,{\rm km\,s^{-1}}$, differs considerably from the published value, $-49\,{\rm km\,s^{-1}}$ (Boulon 1963). While the unspecified precision of this determination, based on an objective prism spectrum, must be limited, consideration of, for instance, Fig. 35 of this reference supports the view that the change between the two epochs is highly significant and hence indicative of previously unreported binarity. Some of the sharpest lines visible in the HARPS-N spectrum, including a couple of the Fe I lines that we used to diagnose $\langle B_{\rm q} \rangle$, have depths exceeding 0.9: the companion star does not contribute significantly to the observed spectrum. It must be much fainter than the Ap component.

5. Summary

Table 1, which is similar to Table 1 of M24, summarises the results of our analysis. For ten of the studied stars, the projected equatorial velocity definitely appears consistent with super-slow rotation. Six are ssrAp star candidates for which the conclusion drawn from our TESS survey receives independent confirmation. A seventh one (HD 17330) had already been confirmed by M24. For the remaining three, values of the rotation period $P_{\rm rot} > 50 \,\mathrm{d}$ were available in the literature. For six more stars (including two already considered in M24), the derived upper limit of $v \sin i$ could indicate either super-slow rotation or a moderately long period (20 d $\lesssim P_{\rm rot} \lesssim 50$ d), while HD 89069 almost certainly has a moderately long rotation period. While one could in principle compute minimum values of the rotation period of each star by combining the derived upper limit of $v \sin i$ with a radius value (available from the literature), we prefer to avoid this to also take into account our assessment of the reliability of $(v \sin i)_{\text{max}}$ – for instance, to which extent it may be affected by crosstalk between the various line broadening terms in the regression analysis. Even though this approach involves a degree of subjectivity, it reduces the risk of overinterpretation of unqualified numerical values. As previously mentioned, we prefer to postpone the accurate determination of $v \sin i$ and of a corresponding limit of P_{rot} to a future detailed analysis of stars for which multi-epoch observations confirm without ambiguity the occurrence of super-slow rotation.

Seventeen of the 18 stars of this study are definitely magnetic. For five of them, detection is achieved here for the first time. No formally significant value of the magnetic field could be determined for the eighteenth star, BD+35 5094, but its spectrum is indicative of differential broadening of lines of different magnetic sensitivity. For two of the stars, HD 8441 and HD 11187, the presence of the magnetic field is inferred from mean longitudinal magnetic field measurements from the literature. Formally significant values of the mean quadratic magnetic field were derived for the remaining 15. The occurrence of resolved magnetically split lines in the visible spectrum of five stars is reported here for the first time. In total, eleven of the 18 stars of this study show magnetic resolution of the Fe II λ 6149.2 Å line, making it possible to determine their mean magnetic field modulus

At least eight, and probably nine of the analysed stars are spectroscopic binaries. The binarity of five of them does not seem to have been reported before (although, for BD+35 5094, different radial velocity values had been published). The binarity of HD 89069 was suspected, but it needs to be confirmed through additional precise measurements.

6. Conclusion

The main purpose of the study presented in M24 and in this paper was to obtain spectroscopic confirmation of the viability of the ssrAp star candidates identified photometrically by Mathys et al. (2020, 2022, 2024b), for which no relevant information about the rotation period or the projected equatorial velocity was found in the literature. We have now completed the acquisition of the spectra of all but two such stars with magnitude $V \leq 9.5$. Upon visual inspection, a fraction of them definitely show rotational line broadening incompatible with values of the rotation period $P_{\rm rot} > 50 \,\mathrm{d}$. We provisionally left them aside, postponing to a later stage the investigation of the reasons why no photometric variability on rotational time scales shorter than ~20 d were found in our TESS survey. The analysis of the spectra obtained as part of our project for the remaining ssrAp star candidates is now complete. Not only have we determined upper limits of the projected equatorial velocities of the observed stars, but also we have performed first measurements of their magnetic fields and, in a number of cases, we have been able to test their possible binarity. The outcome represents a valuable basis to derive constraints on the distribution of the rotation rates and on the connections between slow rotation and other physical parameters.

Nevertheless, it would be premature at this stage to undertake such an endeavour, because there is still both in our files and in observatory archives a wealth of unexploited spectroscopic material available about those stars for which information supporting the identification as ssrAp star candidates exists in the literature. For many of these stars, the existing observational material can be used to extract constraints about the rotational velocity, the magnetic field, and/or the binarity, that have not been considered until now. By carrying out this task as the next step of our project, we shall build a more exhaustive database that will put us in the position to explore the connections between long rotation periods and other stellar properties in a more statistically significant manner than if we limited ourselves to the data obtained by us that we have analysed until now.

On the other hand, the 16 stars listed in Table 1 under 'ssrAp stars' or 'Long period Ap stars' fulfil the necessary condition of low enough projected equatorial velocity to be ssrAp stars. However, only three of them have been confirmed until now to have rotation periods $P_{\rm rot} \gtrsim 50$ d. Determination of the periods of the remaining 13 is required to ascertain their rotational status. In most cases, this will be best done by studying the variability of their magnetic field (Mathys 2020). The most suitable strategies to this effect have been discussed in detail in M24. Their implementation, which represents one of the next steps of our project, is already in progress.

Data availability

HARPS-N, SALT-HRS, UVES, HARPS, and FEROS reduced spectra are available at the CDS via https://cdsarc.cds.unistra.fr/viz-bin/cat/J/A+A/703/A102.

Acknowledgements. Based on observations made with the Italian Telescopio Nazionale Galileo (TNG) operated on the island of La Palma by the Fundación Galileo Galilei of the INAF (Istituto Nazionale di Astrofisica) at the Spanish Observatorio del Roque de los Muchachos of the Instituto de Astrofisica de Canarias; on observations obtained with the Southern African Large Telescope under the proposal codes 2022-2-SCI-017, 2024-1-SCI-007, 2024-2-SCI-023

(PI: Holdsworth); on observations collected at the European Southern Observatory under ESO programme 078.D-0080; and on processed data obtained from the ESO Science Archive Facility. This work has made use of the VALD database, operated at Uppsala University, the Institute of Astronomy RAS in Moscow, and the University of Vienna. This research has also made use of the SIMBAD database, operated at CDS, Strasbourg, France.

References

```
Aurière, M., Wade, G. A., Silvester, J., et al. 2007, A&A, 475, 1053
Babcock, H. W. 1958, ApJS, 3, 141
Boulon, J. 1963, Journal des Observateurs, 46, 243
Bramall, D. G., Sharples, R., Tyas, L., et al. 2010, in Proc. SPIE, SPIE Conf.
   Ser., 7735, 77354F
Burke, E. W., Jr, & Lady, S. 1977, Inf. Bull. Var. Stars, 1288, 1
Carrier, F., North, P., Udry, S., & Babel, J. 2002, A&A, 394, 151
Chojnowski, S. D., Hubrig, S., Hasselquist, S., et al. 2019, ApJ, 873, L5
Cosentino, R., Lovis, C., Pepe, F., et al. 2012, in Ground-based and Airborne
   Instrumentation for Astronomy IV, eds. I. S. McLean, S. K. Ramsay, & H.
   Takami, SPIE Conf. Ser., 8446, 84461V
Dekker, H., D'Odorico, S., Kaufer, A., Delabre, B., & Kotzlowski, H. 2000, in
   Optical and IR Telescope Instrumentation and Detectors, eds. M. Iye, & A. F.
   Moorwood, SPIE Conf. Ser., 4008, 534
Elkin, V. G., Kurtz, D. W., Mathys, G., & Freyhammer, L. M. 2010, MNRAS,
   404, L104
Elkin, V. G., Kurtz, D. W., & Nitschelm, C. 2012, MNRAS, 420, 2727
Ferrario, L., Pringle, J. E., Tout, C. A., & Wickramasinghe, D. T. 2009, MNRAS,
Freyhammer, L. M., Elkin, V. G., Kurtz, D. W., Mathys, G., & Martinez, P. 2008,
   MNRAS, 389, 441
Gaia Collaboration (Brown, A. G. A., et al.) 2018, A&A, 616, A1
Gaia Collaboration (Arenou, F., et al.) 2023, A&A, 674, A34
Giarrusso, M., Cecconi, M., Cosentino, R., et al. 2022, MNRAS, 514, 3485
Gontcharov, G. A. 2006, Astron. Lett., 32, 759
Holdsworth, D. L., Cunha, M. S., Kurtz, D. W., et al. 2021, MNRAS, 506, 1073
Hubrig, S., Chojnowski, S. D., Järvinen, S. P., Ilyin, I., & Pan, K. 2024, A&A,
   687, A282
Kaufer, A., Stahl, O., Tubbesing, S., et al. 1999, The Messenger, 95, 8
Kochukhov, O., Alentiev, D., Ryabchikova, T., et al. 2013, MNRAS, 431, 2808
Leone, F., Avila, G., Bellassai, G., et al. 2016, AJ, 151, 116
Martinez, P. 1993, Ph.D. Thesis, University of Cape Town (South Africa)
Mathys, G. 1995, A&A, 293, 746
Mathys, G. 2017, A&A, 601, A14
Mathys, G. 2020, in Stellar Magnetism: A Workshop in Honour of the Career and
   Contributions of John D. Landstreet, eds. G. Wade, E. Alecian, D. Bohlender,
   & A. Sigut, 11, 35
Mathys, G., & Hubrig, S. 2006, A&A, 453, 699
Mathys, G., Hubrig, S., Landstreet, J. D., Lanz, T., & Manfroid, J. 1997, A&AS,
Mathys, G., Kurtz, D. W., & Holdsworth, D. L. 2020, A&A, 639, A31
Mathys, G., Kurtz, D. W., & Holdsworth, D. L. 2022, A&A, 660, A70
Mathys, G., Holdsworth, D. L., Giarrusso, M., et al. 2024a, A&A, 691, A186
Mathys, G., Holdsworth, D. L., & Kurtz, D. W. 2024b, A&A, 683, A227
Mathys, G., Holdsworth, D. L., Giarrusso, M., et al. 2025, A&A, 694, C7
Mayor, M., Pepe, F., Queloz, D., et al. 2003, The Messenger, 114, 20
North, P., Carquillat, J.-M., Ginestet, N., Carrier, F., & Udry, S. 1998, A&AS,
   130, 223
Preston, G. W. 1971, ApJ, 164, 309
Pyper, D. M., & Adelman, S. J. 2017, PASP, 129, 104203
Ricker, G. R., Winn, J. N., Vanderspek, R., et al. 2015, J. Astron. Telesc., Instrum.
   Syst., 1, 014003
Romanyuk, I. I., Semenko, E. A., Kudryavtsev, D. O., Moiseeva, A. V., &
   Yakunin, I. A. 2017, Astrophys. Bull., 72, 391
```

Romanyuk, I. I., Semenko, E. A., Moiseeva, A. V., Kudryavtsev, D. O., &

Romanyuk, I. I., Moiseeva, A. V., Semenko, E. A., Kudryavtsev, D. O., &

Titarenko, A. R., Semenko, E. A., & Ryabchikova, T. A. 2012, Astron. Lett., 38,

Shultz, M. E., Wade, G. A., Rivinius, T., et al. 2018, MNRAS, 475, 5144

Shultz, M. E., Wade, G. A., Rivinius, T., et al. 2019, MNRAS, 490, 274 Steinmetz, M., Guiglion, G., McMillan, P. J., et al. 2020, AJ, 160, 83

Tutukov, A. V., & Fedorova, A. V. 2010, Astron. Rep., 54, 156

Yakunin, I. A. 2018, Astrophys. Bull., 73, 178

Yakunin, I. A. 2020, Astrophys. Bull., 75, 294

Appendix A: Observations and measurements

Table A.1. Measurements of the spectra of the ssrAp star candidates.

TIC	Other ID	V	HJD (2,400,000.+)	Instr	S/N	T _{eff} (K)	$v_{\rm r}$ $({\rm kms^{-1}})$	$\frac{\sigma(v_{\rm r})}{({\rm km~s^{-1}})}$	⟨ <i>B</i> ⟩ (G)	$\begin{array}{c} \sigma(\langle B \rangle) \\ \text{(G)} \end{array}$	$N_{ m g}$	$\langle B_{\rm q} \rangle$ (G)	$\sigma(\langle B_{\mathbf{q}} \rangle)$ (G)	N_l	$ (v \sin i)_{\text{max}} $ $ (km s^{-1}) $	$\frac{\sigma(v\sini)}{(\mathrm{kms^{-1}})}$
32259138	HD 138777	9.73	60432.570	S	150	7352	-43.72	0.12	4698	100	3	5600	300	46	_	
88202438	HD 192686	8.88	60540.457	N	85	11670	-10.30	0.05	3573	50	2	4730	230	64	_	
93522454	HD 143487	9.43	54140.822	F	170	7114			4216	100	3	3940	780	21	5.8	0.8
			54173.913	U	180		-23.36	0.69	4153	60	3	2630	920	17	7.5	1.4
			54535.850	U	135		-14.00		4111	60	3	2890	750	17	7.5	1.4
			54536.815	U	225		-14.24		4111	60	3	3280	630	17	7.5	1.4
			55374.730	U	325		-25.20		4195	60	3	3330	760	14	7.5	1.4
			55609.836	Н	50		-22.27		4006	100	3	4220	1250	19	6.9	1.3
			60032.483	S	220		-18.11	0.41	4467	100	3	4330	1350	18	5.8	1.3
163801263	HD 203922	8.50	60539.473	N	75	7602	-23.92	0.05	3503	30	2	3830	120	78	2.9	0.2
170419024	HD 151860	9.01	55326.858	U	390	6625	3.45		2265	40	2	2580	170	26	4.2	0.3
238659021	HD 8441	6.68	60686.361	N	160	9205	3.68	0.03				_		64	3.1	0.2
251976407	HD 221568	7.55	60686.313	N	125	9472	-8.33	0.12	2433	30	2	2790	250	38	_	
301918605	HD 17330	7.11	60686.421	N	240	10250	-12.42	0.03				1130	180	72	1.4	0.1
341616734	HD 89069	8.42	60663.707	N	100	9546	-9.23	0.10				3380	120	83	4.3	0.2
			60686.678	N	100		-9.17	0.05				3200	90	78	4.8	0.1
352787151	BD+35 5094	9.08	60686.350	N	85	6900	-6.81	0.05				-		85	2.0	0.2
356088697	HD 76460	9.80	55227.707	F	270	7110			3607	40	2	3890	260	64	4.0	0.3
			60038.395	S	210		2.20	0.11	3586	50	2	3350	340	60	3.9	0.4
369969602	HD 128472	9.87	60484.425	S	210	7259	-16.94	0.15				1840	570	46	3.3	0.4
380607580	HD 119794	9.00	60704.562	S	145	9347	-21.49	0.16	5369	40	2	4800	400	47	6.1	0.5
403625657	HD 11187	7.94	60539.704	N	65	10750	5.73	0.06				-		49	15.3	0.1
405516045	HD 110274	9.47	54138.884	F	180	7766			3775	40	3	3580	440	39	2.5	0.5
			54141.828	F	100		-1.43	0.10	3754	40	3	3350	370	42	4.1	0.4
			54172.906	U	150		-7.75	0.08	5034	30	2	6320	150	33	_	
			54523.854	U	115		-2.97	0.08	4698	30	2	6000	170	33	-	
			54535.815	U	170		-4.94	0.09	4425	30	2	5670	200	33	1.5	0.5
			60032.587	S	250		-1.49	0.14	5243	40	2	5850	260	38	3.2	0.4
419916333	HD 117290	9.25	54139.763	F	160	7271			6439	40	2	7320	330	21	-	
			54141.866	F	130		-27.57		6313	40	2	7540	310	22	_	
			54171.921	U	120		-26.97		6334	30	2	7650	260	27	_	
			54515.870 60036.350	U S	250 260		-4.47 -36.87	0.15	4509 3020	30 40	2	6550 2630	270 630	27 34	2.2	0.7
120255005	DD : 50 2124	10.12				0066										
	BD+52 3124		60540.656	N	50	9066	-10.94		4237	50	2	4920	170	55	2.3	0.4
470837956	BD+61 2565	9.9	60555.089	N	200	8178	-17.89	0.06				1680	140	111	2.4	0.2

Notes. The stars are listed in order of increasing TIC (TESS Input Catalogue) number (Col. 1), with another ID (preferably the HD number) given in Col. 2 and the V magnitude in Col. 3. The Heliocentric Julian Date (HJD) of mid-observation, the instrument with which it was obtained (F = FEROS; H = HARPS; N = HARPS-N; S = SALT-HRS; U = UVES), and the resulting S/N appear in Cols. 4 to 6. The values of T_{eff} in Col. 7 are from the TIC (they are listed as published there even though effective temperatures cannot be determined with 1 K precision). The following columns contain the results of our measurements: the stellar radial velocity v_r and its uncertainty $\sigma(v_r)$ (Cols. 8 and 9; the entries were left blank when these values could not be determined); the mean magnetic field modulus $\langle B \rangle$, its uncertainty $\sigma(\langle B \rangle)$, and the number N_g of Gaussians fitted to the Fe II λ 6149.2 Å line for its determination (Cols. 10 to 12); the mean quadratic magnetic field $\langle B_q \rangle$, its formal uncertainty $\sigma(\langle B_q \rangle)$, and the number N_l of diagnostic lines from which it was derived (Cols. 13 to 15); the upper limit ($v \sin i v_{\text{max}}$) of the projected equatorial velocity and the formal uncertainty $\sigma(v \sin i)$ of the $v \sin i$ determination (Cols. 16 and 17). The values of the radial velocity and of the projected equatorial velocity are derived from analysis of the same sample of N_l lines as used for the $\langle B_q \rangle$ determination. For spectra in which the Fe II λ 6149.2 Å line is not resolved into its magnetic field is below the detection threshold, and in Col. 14, those spectra in which the rotational Doppler broadening is below the detection threshold. (For TIC 93522454, the $\langle B_q \rangle$ value derived from the first UVES spectrum was given as it is only marginally below the formal detection threshold and as significant values of similar order were determined from the other UVES observations of this star.)

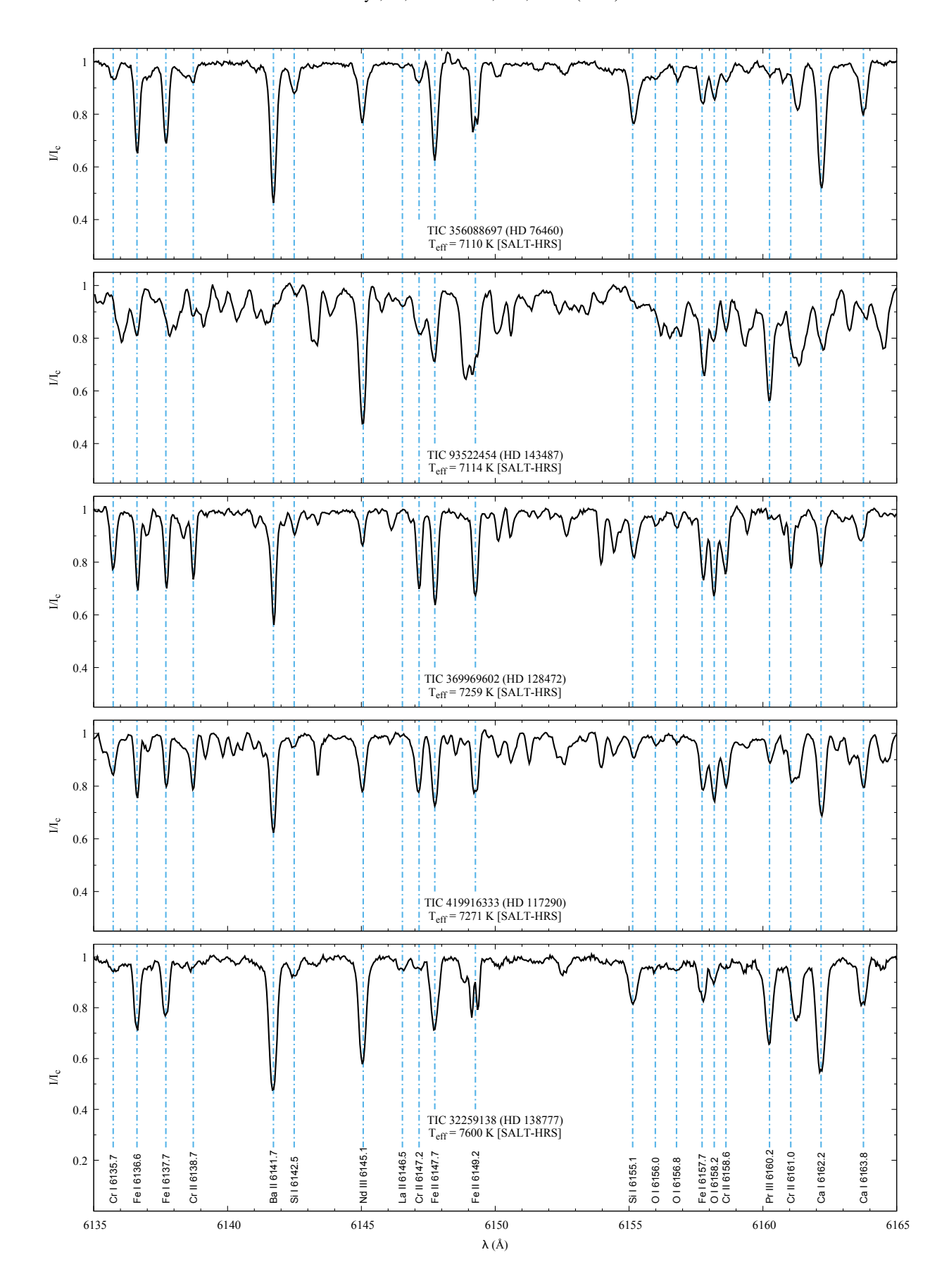


Fig. A.1. Portion of the spectrum of five sharp-lined ssrAp star candidates. The wavelengths are in the laboratory reference frame.

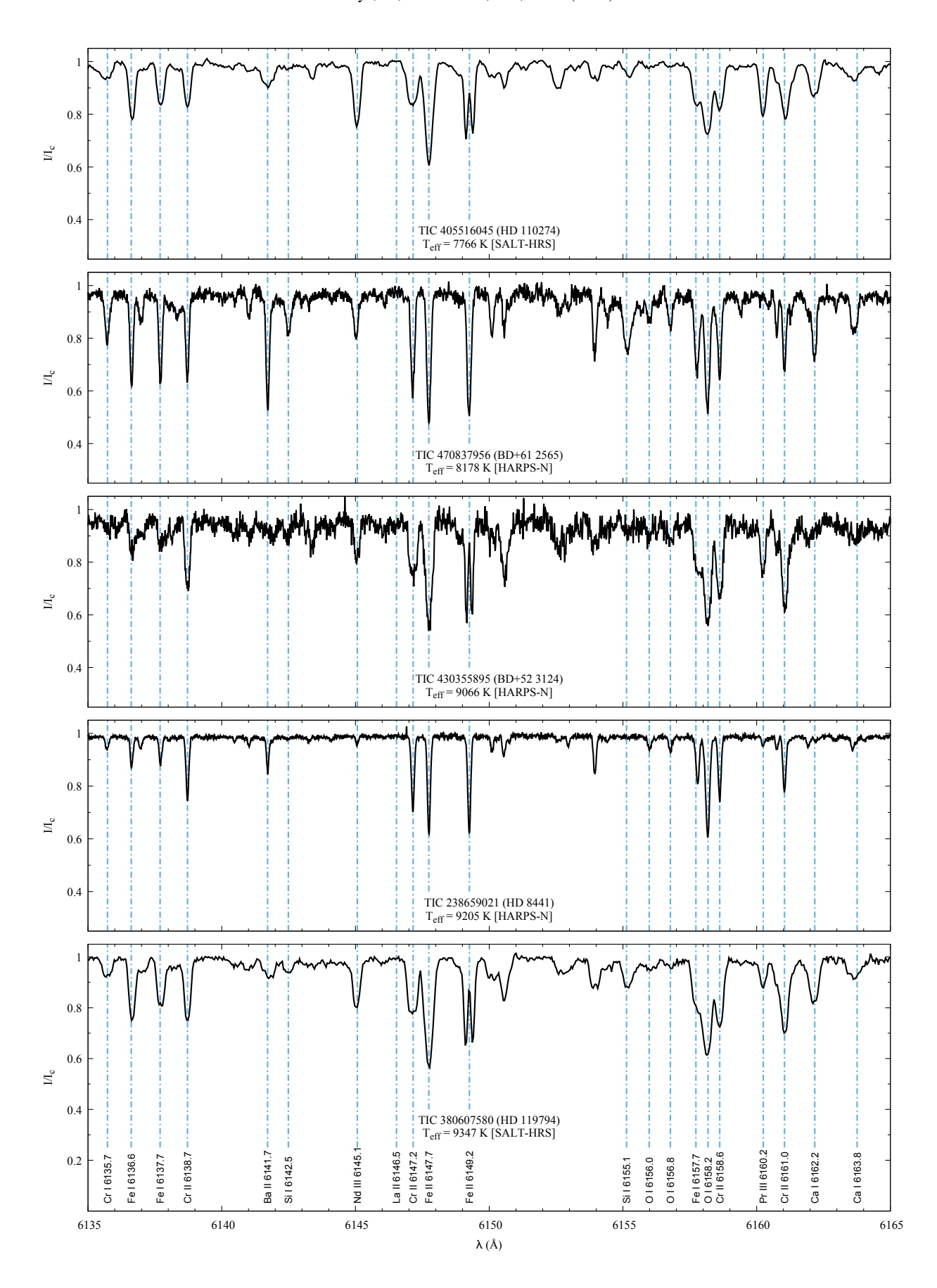


Fig. A.2. Portion of the spectrum of five sharp-lined ssrAp star candidates. The wavelengths are in the laboratory reference frame.

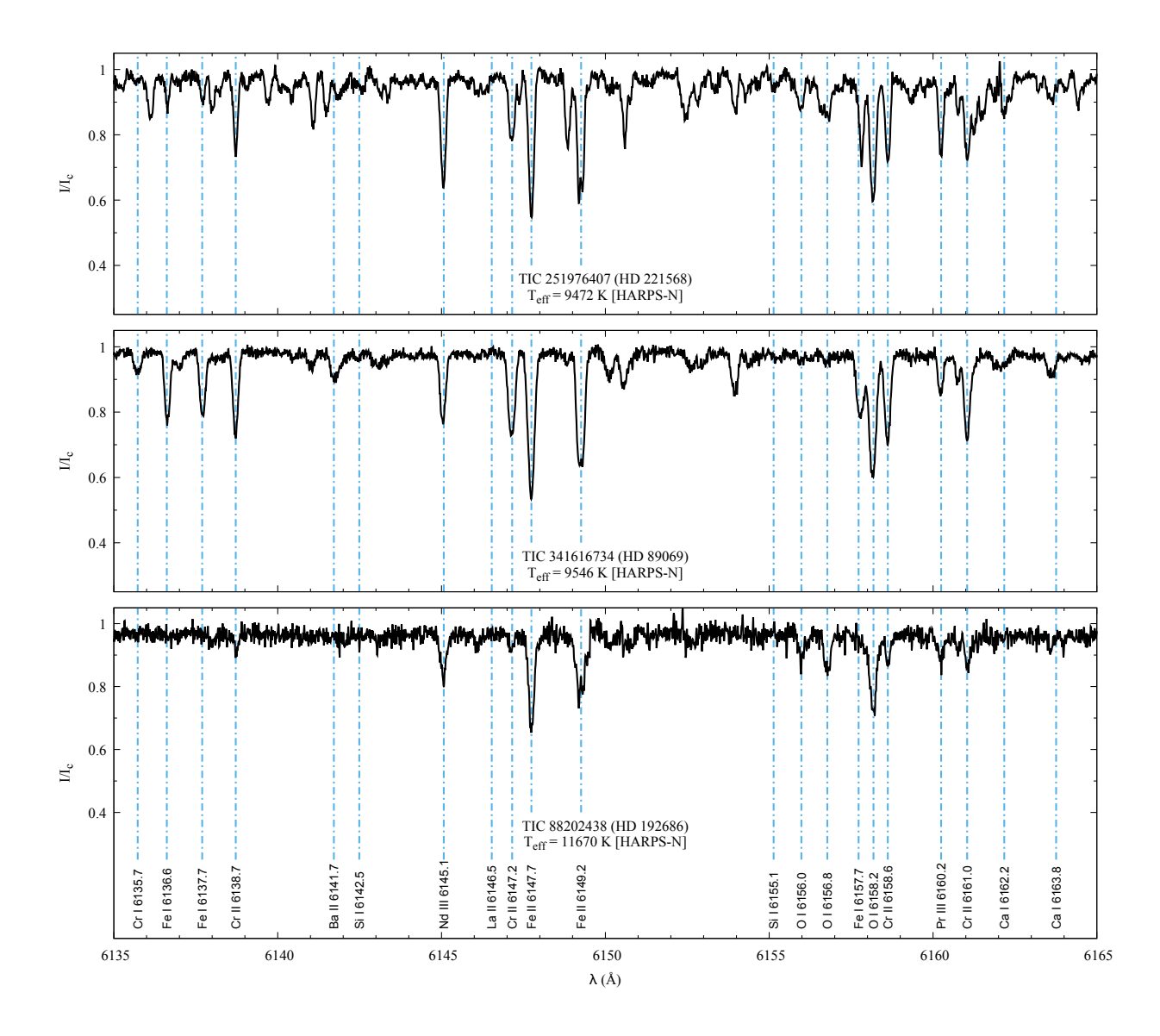


Fig. A.3. Portion of the spectrum of three sharp-lined ssrAp star candidates. The wavelengths are in the laboratory reference frame.

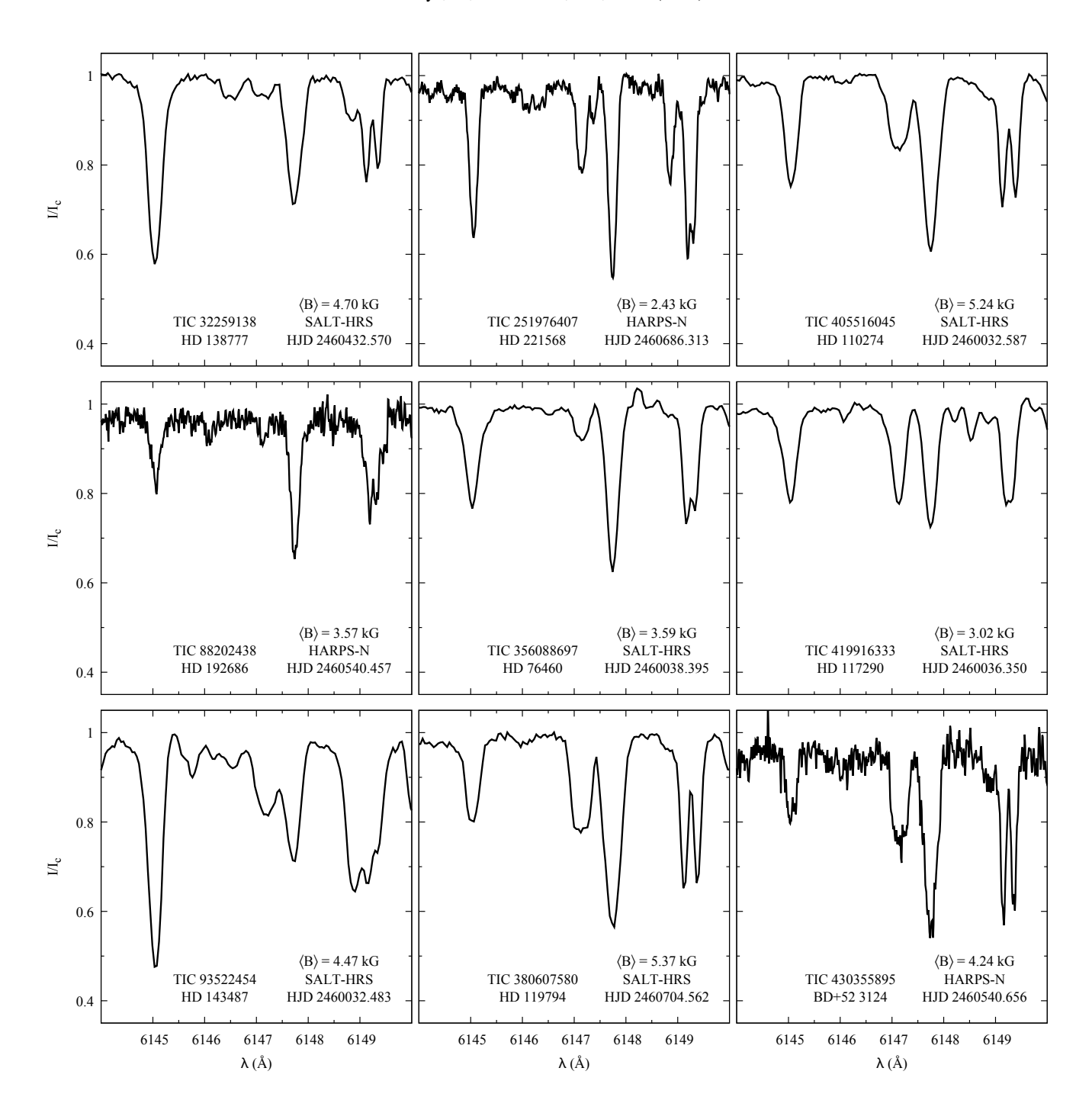


Fig. A.4. Portion of the spectrum of the nine Ap stars with resolved magnetically split lines that were not studied in M24. The wavelengths are in the laboratory reference frame. The main lines are Nd III λ 6145.1 Å, Cr II λ 6147.2 Å, Fe II λ 6147.6 Å, and Fe II λ 6149.2 Å; their Zeeman patterns were shown in Fig. 3 of M24. The doublet pattern of the Fe II λ 6149.2 Å line is of particular interest as it lends itself to mostly approximation-free and model-independent determination of the mean magnetic field modulus $\langle B \rangle$. However, in a fraction of the stars, its blue wing is affected to some extent by blends that may include contributions from the Sm II λ 6149.06 Å line and/or from an unidentified line. This blend is exceptionally strong in HD 143487, which also features the strongest Nd III λ 6145.2 Å line of all the stars shown here. The benefit of the higher resolving power of HARPS-N over the lower one of SALT-HRS for separation of the magnetically split components of the Fe II λ 6149.2 Å line is also apparent in this figure.

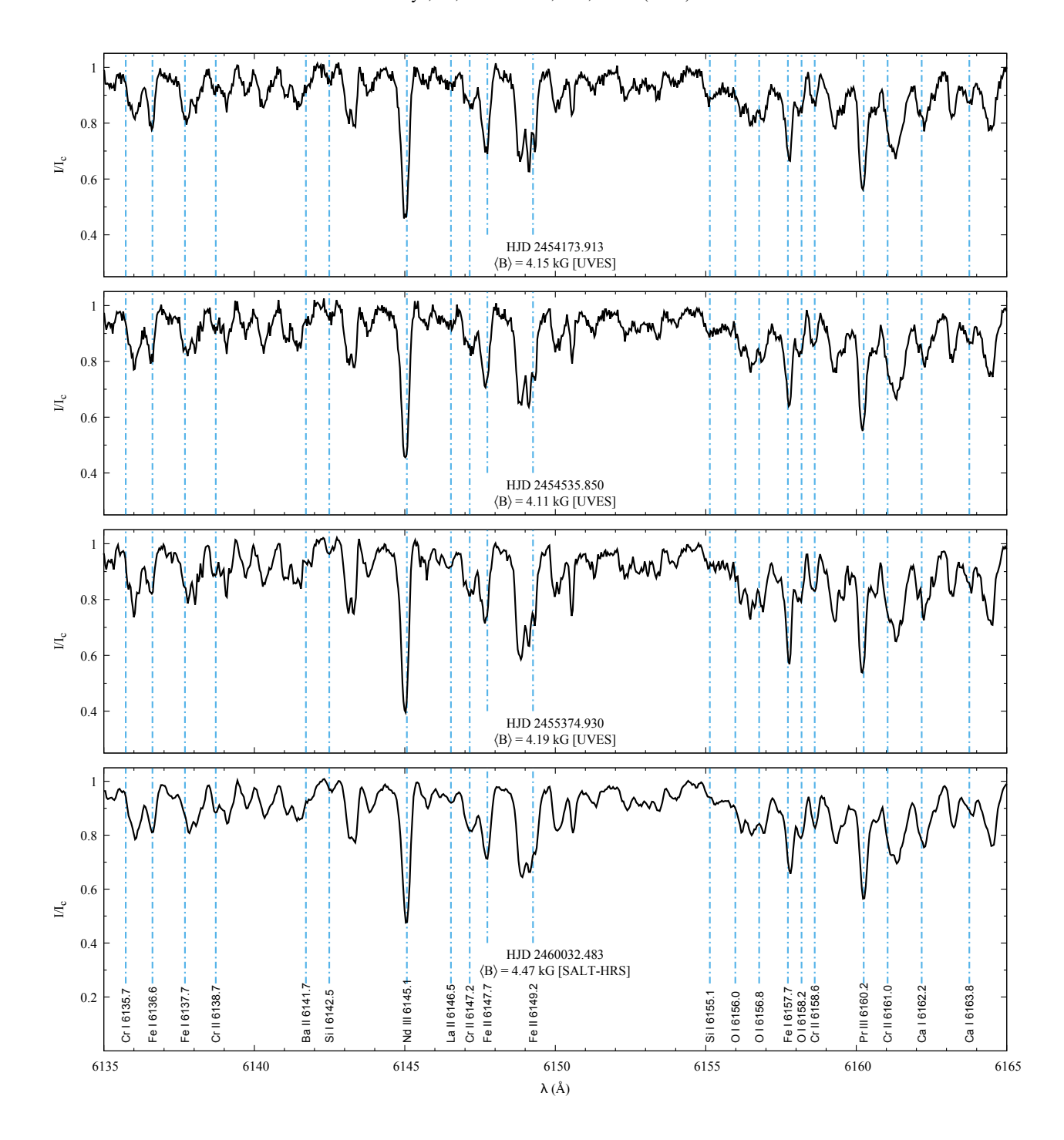


Fig. A.5. Portion of the spectrum of HD 143487 observed at 4 epochs. The wavelengths are in the laboratory reference frame. The same lines as in Figs. A.1 to A.3 are identified even though some may not be seen in the present spectra. The blend affecting the blue side of the Fe II λ 6149.2 Å line, which probably includes a contribution of the Sm II λ 6149.06 Å line in addition to an unidentified line, is deeper than the Fe doublet in the lower (more recent) two spectra than in the upper two. The increase in depth of the Cr II λ 6147.2 Å line from the top to the bottom spectrum is also quite apparent by comparison with the neighbouring Fe II λ 6147.7 Å line. These relative intensity changes in line pairs are suggestive of variations occurring over time scales of years, which is consistent with super-slow rotation.

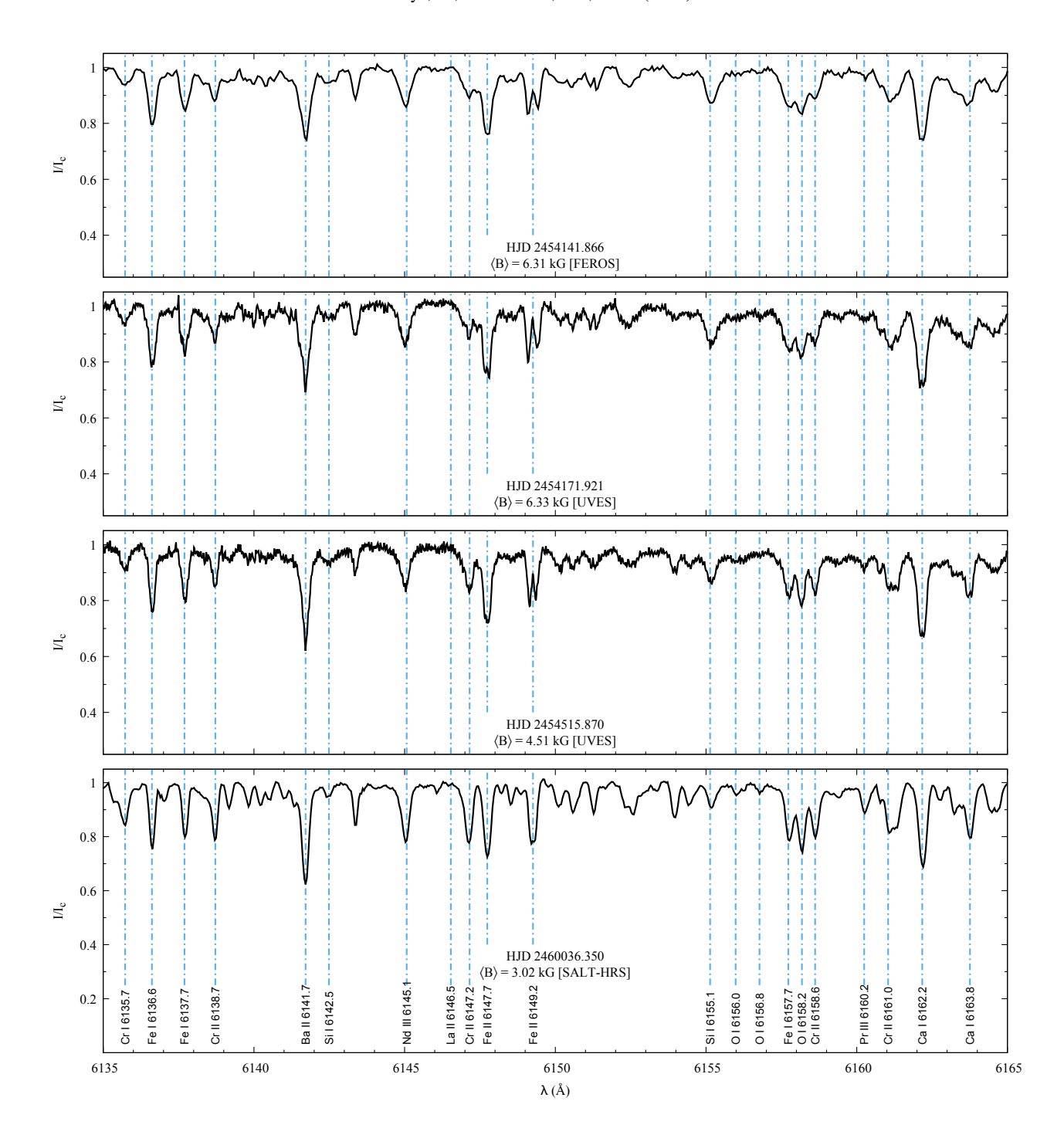


Fig. A.6. Portion of the spectrum of HD 117290 observed at 4 epochs. The wavelengths are in the laboratory reference frame. The same lines as in Figs. A.1 to A.3 are identified even though some may not be seen in the present spectra. The narrowing splitting of the Fe II λ 6149.2 Å line clearly shows the decrease of the mean magnetic field modulus with time. The increase in intensity of the Cr lines from the first observation to the most recent one is particularly notable from comparison of the Cr II λ 6147.2 Å line with the neighbouring Fe II λ 6147.7 Å and λ 6149.2 Å lines. Other Cr lines show similar variations. The strengthening of the Nd III λ 6145.1 Å and Pr III λ 6160.2 Å with weakening $\langle B \rangle$ is also visible. Comparison of the top two spectra, obtained respectively with FEROS and UVES at epochs between which the star did not significantly vary, allows one to assess the effect of the resolution on the line profile appearance.